Asymptotic safety guaranteed at four-loop order

Daniel F. Litim,[1] Nahzaan Riyaz,[1] Emmanuel Stamou,[2] and Tom Steudtner[2,3]

[1]*Department of Physics and Astronomy, University of Sussex, Brighton, BN1 9QH, United Kingdom*
[2]*Fakultät für Physik, TU Dortmund, Otto-Hahn-Strasse 4, D-44221 Dortmund, Germany*
[3]*Department of Physics, University of Cincinnati, Cincinnati, Ohio 45221, USA*

(Received 2 August 2023; accepted 11 September 2023; published 12 October 2023)

We investigate a family of four-dimensional quantum field theories with weakly interacting ultraviolet fixed points up to four-loop order in perturbation theory. Key new ingredients are the three-loop gauge contributions to quartic scalar beta functions, which we compute in the $\overline{\rm MS}$ scheme for a template $SU(N_c)$ gauge theory coupled to N_f fundamental fermions and elementary scalars. We then determine fixed point couplings, field and mass anomalous dimensions, and universal scaling exponents up to the first three nontrivial orders in a small Veneziano parameter. The phase diagram and UV-IR connecting trajectories are found and contrasted with asymptotic freedom. Further, the size of the conformal window, unitarity, and mechanisms leading to the loss of conformality are investigated. Our results provide blueprints for concrete four-dimensional nonsupersymmetric conformal field theories with standard model-like field content and invite further model building.

DOI: 10.1103/PhysRevD.108.076006

I. INTRODUCTION

Ultraviolet (UV) fixed points play a central role for the fundamental definition of quantum field theory (QFT). They ensure that theories are UV-complete, meaning well-defined and predictive up to highest energies. This is quite different from effective field theories that tend to break down above a certain energy. Moreover, and much like critical points in systems with continuous phase transitions, fixed points in particle physics also relate to an underlying conformal field theory (CFT). The existence of free UV fixed points, known as asymptotic freedom, has been established long ago [1,2]. The more recent discovery that high-energy fixed points can also be interacting [3–14], known as asymptotic safety [15,16], has opened up new territory to look for UV-complete extensions of the Standard Model, and for genuinely new phenomena beyond the paradigms of asymptotic freedom or effective field theory [17–36].

A role model for an UV-complete particle theory with a weakly interacting fixed point is given by N_f fermions coupled to $SU(N_c)$ gauge fields and elementary scalars through gauge and Yukawa interactions [3]. Crucially, in the regime where asymptotic freedom is absent, quantum fluctuations ensure that the growth of the gauge coupling is countered by Yukawa couplings, leading to an interacting fixed point in the UV (see Fig. 1). In the large-N limit, the fixed point is under strict perturbative control, and specifics of the theory can be extracted systematically in perturbation theory by using $\epsilon = N_f/N_c - 11/2$ as a small control parameter. Thus far, critical couplings, universal exponents, and the size of the conformal window have been determined up to the second nontrivial order in ϵ, including finite N corrections [3,8,13,17].

In this paper, we extend the study of the UV critical theory to the complete third order in ϵ. The rationale for this is that while the fixed point occurs for the first time at the leading order in ϵ [3], a bound on the UV conformal window $\epsilon < \epsilon_{\rm max}$ arises for the first time at the complete second order in ϵ [8,13]. Thereby, it has also been noted that $\epsilon_{\rm max}$ is numerically small, suggesting that the entire UV conformal window could be within the perturbative domain.[1] The validation of this picture warrants a study up to the third nontrivial order in ϵ. To achieve this goal, the four-loop gauge, three-loop Yukawa and quartic β functions, and three-loop anomalous dimensions are required as input. Some of these can be extracted from generic expressions for beta functions of gauge-Yukawa theories [40,41]. The missing pieces, however, are the three-loop contributions to scalar β functions containing gauge interactions, which we compute using standard

[1]This state of affairs should be compared with the IR conformal window of $SU(N_c)$ gauge theories coupled to N_f fundamental fermions, where the theory becomes strongly coupled; see. for instance. [37–39] and references therein.

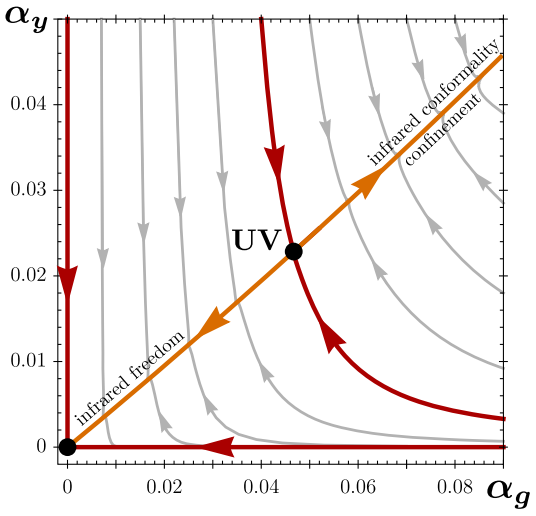

FIG. 1. Phase diagram of an asymptotically safe theory in the gauge-Yukawa plane of couplings (α_g, α_y) at four-loop. Shown are the interacting UV and the free IR fixed points (black dots), and sample trajectories with arrows pointing to the IR. Two asymptotically safe trajectories are running out of the UV fixed point (orange) lead either to infrared freedom at weak coupling, or to confinement or conformality at strong coupling.

techniques in the $\overline{\text{MS}}$ scheme, and which is one of the central results of this work. In addition, we provide fixed point couplings and conformal data of the UV critical theory up to cubic order in ϵ, and look into the loss of conformality, the range of perturbativity, and UV-IR connecting trajectories in comparison with asymptotic freedom.

The paper is organized as follows. Section II recalls the basics of asymptotically safe particle theories, introduces our model, and explains the underlying systematics. In Sec. III, we detail the computation of β functions. In Sec. IV, we present our results, which include beta functions, fixed points, anomalous dimensions and scaling exponents, bounds on the conformal window, and aspects of the phase diagram. We conclude in Sec. V and defer additional material to three appendixes.

II. ASYMPTOTICALLY SAFE GAUGE THEORY

In this section, we recall the basic model and its quantum critical points, as well as the systematics of the underlying perturbative and conformal expansions.

A. Model

We consider a four-dimensional, renormalizable QFT with $SU(N_c)$ gauge group and an unbroken $U(N_f)_L \times U(N_f)_R$ global flavor symmetry. In analogy to massless QCD, the theory features N_f colored, quarklike fermion as well as a complex but uncharged meson-matrix scalar, as listed in Table I. The corresponding Lagrangian

TABLE I. Field content and representations under gauge and global symmetry.

Field		$SU(N_c)$	$U_L(N_f)$	$U_R(N_f)$
Fermion	ψ_L	N_c	N_f	1
	ψ_R	N_c	1	N_f
Scalar	ϕ	1	N_f	$\overline{N_f}$

$$\begin{aligned}\mathcal{L} = &-\frac{1}{4}F^{A\mu\nu}F^{A}_{\mu\nu} + \mathcal{L}_{\text{gf}} + \mathcal{L}_{\text{gh}} + \text{tr}[\bar{\psi} i \not{D} \psi] \\ &- y\,\text{tr}[\bar{\psi}(\phi \mathcal{P}_R + \phi^\dagger \mathcal{P}_L)\psi] + \text{tr}[\partial^\mu \phi^\dagger \partial_\mu \phi] - m^2 \text{tr}[\phi^\dagger \phi] \\ &- u\,\text{tr}[\phi^\dagger \phi \phi^\dagger \phi] - v\,\text{tr}[\phi^\dagger \phi]\text{tr}[\phi^\dagger \phi] \end{aligned} \tag{1}$$

consists of a gauge sector with field strength tensor $F^A{}_{\mu\nu}$, the usual gauge-fixing and ghost terms $\mathcal{L}_{\text{gf}}$ and $\mathcal{L}_{\text{gh}}$, and the coupling to the fermions via the covariant derivative D_μ and the gauge coupling g. Traces in (1) run over both flavor and gauge indices. Crosstalk between the scalar and gauge sector is mediated via the real Yukawa coupling y. This interaction is manifestly chiral due to the projectors $\mathcal{P}_{R,L} = \frac{1}{2}(1 \pm \gamma_5)$. In the scalar sector, we observe real-valued single-trace (u) and double-trace quartic couplings (v). The scalar mass term in (1) is compatible with the global symmetry of the model. Below, we are mostly interested in the massless limit.

B. Veneziano limit

In this work, we are interested in the planar (Veneziano) limit [42], where field multiplicities N_f and N_c are large and interactions are parametrically weak. The virtue of the Venziano limit is that it offers rigorous perturbative control, allowing systematic expansions in a small parameter. To prepare for the Veneziano limit, we introduce rescaled couplings [43]

$$\alpha_x = \frac{N_c x^2}{(4\pi)^2}, \qquad \alpha_u = \frac{N_f u}{(4\pi)^2}, \qquad \alpha_v = \frac{N_f^2 v}{(4\pi)^2}, \tag{2}$$

where $x = g, y$. Notice that the gauge, Yukawa, and single-trace scalar couplings scale linearly, while the double-trace scalar couplings scale quadratically with matter field multiplicity. In the Veneziano limit, any explicit dependence on (N_c, N_f) drops out after the rescaling (2), and leaves us with a dependence on ϵ,

$$\epsilon \equiv \frac{N_f}{N_c} - \frac{11}{2}. \tag{3}$$

Moreover, the parameter (3) becomes continuous in this limit, taking values in the entire range $\epsilon \in [-\frac{11}{2}, \infty)$. We are particularly interested in the regime

$$|\epsilon| \ll 1, \tag{4}$$

where it serves as a small control parameter for perturbativity. The virtue of the parameter (3) is that it is proportional to the one-loop coefficient of the gauge beta function, which is at the root for perturbatively controlled fixed points in any four-dimensional (4D) quantum field theory [4,5].

This last point can be illustrated, exemplarily, by expanding a gauge beta function to second-loop order,

$$\beta_g|_{\text{null}} = \frac{4}{3}\epsilon\alpha_g^2 + C\alpha_g^3 + \mathcal{O}(\epsilon\alpha_g^3, \alpha_g^4). \tag{5}$$

If other couplings α_i are present, we project them onto their nullclines ($\beta_i = 0$). The coefficient C, generically of order unity, relates to the gauge two-loop coefficient, possibly modified through Yukawa interactions by the nullcline projection [4]. Consequently, a nontrivial fixed point arises from a cancellation between the parametrically suppressed one-loop term and the two-loop term,

$$\alpha_g^* = -\frac{4\epsilon}{3C} + \mathcal{O}(\epsilon^2), \tag{6}$$

leading to a power series in the control parameter ϵ, with higher order loop terms leading to subleading corrections in ϵ.[2] If other couplings are present, the nullcline conditions dictate that their fixed points are $\alpha_i^* \propto \alpha_g^*$. We conclude that strict perturbativity of fixed points in non-Abelian gauge theories can always be guaranteed for sufficiently small $\epsilon \to 0$ [4,5]. For examples of gauge theories where interacting UV fixed points exist nonperturbatively, including away from a Veneziano limit and at large ϵ, we refer to [14].

C. Systematics

A key feature of non-Abelian gauge theories coupled to matter is that fixed point couplings α_i^* (2) can be systematically expanded as a power series in the small parameter ϵ [8]. For our setting, this implies the "conformal expansion" in powers of ϵ,

$$\alpha_i^* = \sum_{n=1}^{\infty} \alpha_i^{(n)} \epsilon^n \quad (i = g, y, u, v). \tag{7}$$

The expansion coefficients $\alpha_i^{(n)}$ are determined using perturbation theory. To obtain all fixed point couplings (7) accurately up to and including the order ϵ^n, the perturbative loop expansion must be performed up to the loop order $n+1$ in the gauge, and up to order n in the Yukawa and quartic beta functions, to which we refer as the $(n+1)nn$ approximation [8].[3] Ultimately, the reason why the systematics of the perturbatively-controlled expansion requires one more loop order in the gauge sector is that the one-loop gauge coefficient is parametrically as large as the gauge two-loop coefficient. This result establishes a link between the perturbative loop expansion and the conformal expansion in ϵ. The leading order ϵ^0 (LO) relates to the loop order 100, where the running gauge coupling is parametrically slowed down but a fixed point cannot (yet) arise. The next-to-leading order ϵ^1 (NLO), corresponding to 211, offers the first nontrivial order where a fixed point materializes [3], and the next-to-next-to-leading order ϵ^2 (2NLO), corresponding to 322, is the first nontrivial order where bounds on the conformal window arise [8,13]. In this work, we provide the order ϵ^3 (3NLO) corresponding to the 433 approximation.

D. Fixed points

We briefly recall the weakly interacting fixed points of the theory (1). For $\epsilon < 0$, the theory is asymptotically free [1,2], and one finds the seminal Caswell-Banks-Zaks IR fixed point [44,45] with $\alpha_g^* > 0$ and $\alpha_{y,u,v}^* = 0$. The IR fixed point is known to exist within a conformal window $\epsilon_{\text{min}} < \epsilon < 0$, analogous to the conformal window in QCD with extra fermions. The upper end is determined by the loss of asymptotic freedom. The fixed point becomes strongly coupled at the lower end $\epsilon = \epsilon_{\text{min}}$. The exact value for $\epsilon_{\text{min}} > -\frac{11}{2}$, however, is not established with high accuracy (see, for instance, [38,39] and references therein). Also, in the regime with asymptotic freedom, the theory does not exhibit a perturbatively controlled fixed point with nontrivial Yukawa interactions $\alpha_y^* \neq 0$ [4]. These main characteristics are illustrated in Fig. 2.

For $\epsilon > 0$, on the other hand, asymptotic freedom is absent. Then, a UV completion requires the appearance of an interacting UV fixed point. Most importantly, such a phenomenon necessitates a delicate interplay of non-Abelian gauge, Yukawa, and scalar interactions, and cannot arise from gauge interactions alone [4,5]. It then gives rise to a fully interacting UV fixed point ($\alpha_{g,y,u,v}^* \neq 0$) [3,17] and a conformal window $0 < \epsilon < \epsilon_{\text{max}}$.

This UV fixed point and its renormalization group (RG) flow in the (α_g, α_y) plane are shown in Fig. 1. In the vicinity the UV fixed point, the RG flow is power law rather than logarithmic, with respect to the renormalization scale μ,

$$\alpha_i = \alpha_i^* + \sum_j c_{i,j} \left(\frac{\mu}{\mu_0}\right)^{\vartheta_j}, \tag{8}$$

[2]Physicality of the fixed point requires that $\epsilon \cdot C < 0$.

[3]For want of terminology, we denote settings which retain the gauge/Yukawa/quartic beta functions up to the $l/m/n$ loop order as the "lmn approximation."

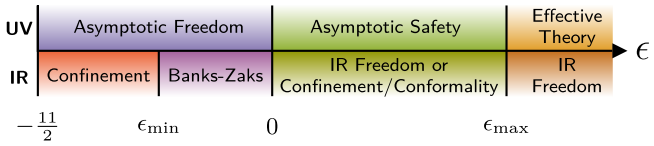

FIG. 2. Main characteristics of the theory (1) as a function of the Veneziano parameter ϵ. In the UV, we indicate whether the theory is asymptotically free, safe, or UV-incomplete and described by an effective field theory. In the IR, we indicate whether the theory achieves confinement, IR freedom, or an interacting conformal fixed point.

characterized by universal scaling exponents ϑ. The sign of the critical exponents ϑ_i in (8) determines whether an RG trajectory connects to the fixed point in the UV or IR, in which case it is called relevant or irrelevant, respectively. While there are three irrelevant eigendirections, only one RG trajectory reaches the fixed point in the UV. Thus, asymptotic safety is established along a one-dimensional submanifold in parameter space. Emanating from the UV fixed point, the two outgoing trajectories lead either to IR freedom or toward a strongly coupled regime with either confinement or an interacting conformal fixed point. For $\epsilon > \epsilon_{\max}$, the UV fixed point disappears and the theory is described by an effective field theory in the UV, and a free theory in the IR; see Fig. 2 for an illustration of these features.

III. COMPUTING BETA FUNCTIONS

It is the central aim of this work to find and study the renormalization group flow for the theory (1) at the complete 3NLO order in the conformal expansion, which corresponds to the 433 approximation. It requires four-loop $\overline{\text{MS}}$ β functions for the gauge coupling g, as well as the three-loop ones for the Yukawa coupling y, and the scalar quartics u and v. Generic β functions for the gauge and Yukawa couplings have been obtained in Refs. [40,41] using Weyl consistency conditions at 432 [46],[4] while the fully general quartic β functions are available at two-loop order [48,49]. These results are conveniently accessible via software packages such as RGBETA [50] and FORGER [51]. Moreover, quartic and Yukawa contributions to the three-loop β functions for the single- and double-trace quartic couplings u and v have been determined in Refs. [52,53]. Therefore, the only missing pieces for a complete 433 analysis are the three-loop contributions to β_u and β_v containing gauge interactions. Their computation is the main task of this section.

[4]Note that our model (1) is CP-even and cannot generate an additive β function to its topological angle; thus, the caveat raised in Ref. [47] regarding the Weyl consistency condition does not apply.

A. Computational strategy

We have conducted a complete computation of all scalar, fermion, vector-boson, and ghost two-point functions, gauge and Yukawa vertex three-point functions, and scalar four-point functions up to three-loop order. This allows one to compute the $\overline{\text{MS}}$ counterterms that determine all γ and β functions, including the missing three-loop results for the single- and double-trace quartic scalar couplings $\beta_{u,v}$. While we are ultimately interested in the Veneziano limit, our computations have been conducted for finite N_f and N_c.

The calculation has been achieved using the framework MARTIN [54], which has been extended to three-loop order for this purpose. All Feynman diagrams are generated using QGRAF [55] and further evaluated in FORM [56]. Overall, almost 33,500 diagrams have been processed. To distinguish UV and IR poles, we employ the technique of infrared rearrangement (IRA) [57,58]. For convenience, we choose the scalar mass in Eq. (1) to be zero and expand each propagator (with integration momentum p) recursively with a universal mass parameter m_{IRA},

$$\frac{1}{(p-q)^2} = \frac{1}{p^2 - m_{\text{IRA}}^2} + \frac{2p\cdot q - p^2}{p^2 - m_{\text{IRA}}^2}\frac{1}{(p-q)^2}.$$

Finite terms with a sufficiently negative degree of divergence are dropped systematically. To cancel subdivergences in two- and three-loop diagrams, counterterms for scalar and vector-boson masses proportional to m_{IRA}^2 are introduced, while this is not necessary for ghosts or fermions [59]. In the end, the γ matrices along each fermion line either carry Lorentz indices from the gauge boson propagators, or are contracted with the third integration momentum exchanged between the loops. We apply tensor and integration by parts reduction techniques [58], and the program LITERED [60,61] is utilized to reduce all remaining three-loop scalar vacuum integrals to a set of masters [62,63].

B. Treatment of γ_5

Moreover, we would like to comment on the treatment of γ_5, as its naïve definition

$$\{\gamma_5, \gamma^\mu\} = 0, \qquad \gamma_5 = \frac{i}{4!}\varepsilon_{\mu\nu\rho\sigma}\gamma^\mu\gamma^\nu\gamma^\rho\gamma^\sigma \tag{9}$$

with the four-dimensional Levi-Civita symbol ε is in conflict with the dimensional regularization procedure. In fact, this treatment is algebraically inconsistent. In our case, the inconsistencies and ambiguities regarding the γ_5 treatment can only arise starting at three-loops when contracting two different terms $\propto \text{tr}(\gamma^\mu\gamma^\nu\gamma^\rho\gamma^\sigma\gamma_5)$ or with traces of more γ matrices [64], e.g., from diagrams in Fig. 3. As observed in Ref. [46], such terms are only generated if for each closed fermion line ℓ with $n_g^{(\ell)}$ gauge-vertex insertions and $n_y^{(\ell)}$ Yukawa-vertex insertions

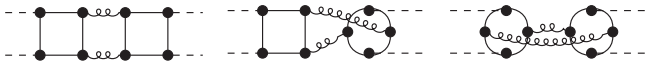

FIG. 3. Scalar four-point diagrams that fulfill Eq. (10), but can still be treated without inconsistencies within the naïve γ_5 scheme as argued in Ref. [59] and discussed in the main text.

$$2n_g^{(\ell)} + n_y^{(\ell)} \geq 5. \tag{10}$$

This constraint cannot be satisfied for scalar two-point functions at three-loop order. There is a single set of scalar four-point diagrams at three-loop where Eq. (10) is fulfilled. These are diagrams containing two fermion loops with $n_y^{(1)} = n_g^{(1)} = n_y^{(2)} = n_g^{(2)} = 2$, as depicted in Fig. 3. Each fermion loop in these diagrams features their own loop momentum, which can be integrated over independently from the rest of the diagram. External momenta can be set to zero as the $1/\varepsilon$ UV pole terms relevant for computing the β functions are independent of them. In the end, the γ matrices along the fermion line are contracted Lorentz indices either from the gauge boson propagators or with the third integration momentum exchanged between the loops. In either case, there are insufficient independent Lorentz indices and momenta feeding into each fermion trace to form a tensor $\propto \mathrm{tr}(\gamma^\mu\gamma^\nu\gamma^\rho\gamma^\sigma\gamma_5)$ [59]. Hence, three-loop quartic β functions, which represent the main result of our computation, cannot depend on the γ_5 scheme and can be treated without inconsistencies within the seminaïve γ_5 scheme employed in this work and discussed below. We extract the four-loop gauge and three-loop Yukawa β functions from literature results [40,41]. In this case it is known that all potential γ_5 ambiguities are fixed due to Weyl consistency conditions [46,65,66].

To deal with γ_5 in our calculation, we employ the seminaïve scheme [59,67] with

$$\{\gamma_5, \gamma^\mu\} = 0, \qquad \gamma_5 = \frac{i}{4!}\tilde{\varepsilon}_{\mu\nu\rho\sigma}\gamma^\mu\gamma^\nu\gamma^\rho\gamma^\sigma, \tag{11}$$

where $\tilde{\varepsilon}$ is a $(4-2\varepsilon)$-dimensional, completely antisymmetric tensor which satisfies the identity

$$\tilde{\varepsilon}^{\mu_1\nu_1\rho_1\sigma_1}\tilde{\varepsilon}_{\mu_2\nu_2\rho_2\sigma_2} = -\delta^{[\mu_1}_{[\mu_2}\delta^{\nu_1}_{\nu_2}\delta^{\rho_1}_{\rho_2}\delta^{\sigma_1]}_{\sigma_2]} + \mathcal{O}(\varepsilon). \tag{12}$$

In exactly four spacetime dimensions, $\tilde{\varepsilon}$ is the Levi-Civita symbol, and the naïve definition in Eq. (9) is recovered. Slightly away from the integer dimension at $d = 4-2\varepsilon$, $\tilde{\varepsilon}$ digresses by terms $\mathcal{O}(\varepsilon)$ from the Levi-Civita case. Hence, the otherwise four-dimensional identity in Eq. (12) picks up corrections $\mathcal{O}(\varepsilon)$. The exact shape of these $\mathcal{O}(\varepsilon)$ corrections is irrelevant for the calculation of counterterms as long as Eq. (12) is only applied in terms that are already finite or only contain a single pole $\frac{1}{\varepsilon}$. We have verified that this is indeed the case in our calculation. Finally, we would like to mention that poles due to non-Hermitian field strength renormalization tensors are absent as the flavor symmetry is unbroken [68–71].

C. Consistency checks

Overall, the computation agrees at finite $N_{f,c}$ with generic literature results [40,41,48,49,72–76] at 432 as well as previous calculations for 433 in the gaugeless limit [52,53]. To cross-check the gauge contributions, we have extended the basis of tensor structures for the general scalar γ and quartic β functions [53] to account for gauge interactions among fermions (while retaining scalars as not charged). Details can be found in Appendix A. Each tensor structure in the general β functions has a universal coefficient that can be determined by comparing the corresponding renormalization group equations of suitable literature results. In our case, we have utilized the three-loop data for the Higgs self-interactions in the SM [59,77–79] with $g_1 = g_2 = 0$, as well as a QED-like gauge-Yukawa theory with a real scalar singlet [80]. All references employ the same seminaïve γ_5 scheme. The literature models are compatible with the generalized Lagrangian (A1). All relevant parts of their scalar quartic β functions, mass, and field anomalous dimensions can be computed using the prescription (A4) and (A5), up to a number of model-independent coefficients. Comparing these results with the explicit computations of [59,77–80] yields relations of those coefficients. Although not all coefficients can be fixed, the data is sufficient to obtain the complete quartic β functions for the theory (1) by using the formalism of (A4) and (A5). We find full agreement with our explicit calculation at finite $N_{f,c}$.

D. Higher orders

To advance the conformal expansion to 4NLO (544 approximation), the complete five-loop gauge as well as four-loop Yukawa and quartic β functions are required. Partial results are available from QCD-like theories [81–86] and from purely scalar theories [52,87]. What is missing, however, are the crucial contributions from Yukawa interactions, the coupling that mediates between the gauge and scalar sectors. It is well-known that Yukawa interactions are key for the primary existence of the fixed point [3–5,88], and their contributions are therefore expected to be equally important at higher orders.

As 544 requires the computation of four-point functions, it is prudent to employ infrared rearrangement by massive propagators as demonstrated in this work. Some tools for this endeavor have already been developed; see, for instance, [89–94] and references therein. However, and given the limitations of the seminaïve algorithm, the main new complication will be the consistent treatment of γ_5. Notice that up until now this has not been an issue in QCD-like or purely scalar theories. Also, while at 432 all γ_5-ambiguities have been removed using Weyl consistency

conditions [46,65], it is far from evident that the same can be achieved at higher orders. For starters, this would require the formulation of a basis for generalized 543 and 654 β functions, which in itself is a massive undertaking. We also point out that a complete basis for the general quartic β function at three-loops does not yet exist. These ambitious endeavors are left for future work.

IV. RESULTS

In this section, we summarize our results for beta functions and anomalous dimensions, and determine fixed points and universal scaling dimensions up to the third nontrivial order in the Veneziano parameter. We also discuss aspects of unitarity, bounds on the conformal window, and the phase diagram and UV-IR connecting trajectories in comparison with asymptotic freedom.

A. Beta functions

In this section we list the β functions in the loop expansion

$$\beta_i \equiv \frac{\mathrm{d}\alpha_i}{\mathrm{d}\ln\mu} = \sum_{\ell=1}^{\infty} \beta_i^{(\ell)}, \tag{13}$$

with $i = g,\ y,\ u,\ v$. The new pieces with respect to the previous analysis [8] are the four-loop contributions to the gauge $\beta_g^{(4)}$, the three-loop contribution to the Yukawa $\beta_y^{(3)}$, and the three-loop contributions to the scalar beta functions $\beta_{u,v}^{(3)}$. Specifically,

$$\begin{aligned}
\beta_g^{(1)} &= \frac{4}{3}\epsilon\alpha_g^2,\\
\beta_g^{(2)} &= \left(25+\frac{26}{3}\epsilon\right)\alpha_g^3 - \frac{1}{2}(11+2\epsilon)^2\alpha_y\alpha_g^2,\\
\beta_g^{(3)} &= \left(\frac{701}{6}+\frac{53}{3}\epsilon-\frac{112}{27}\epsilon^2\right)\alpha_g^4 - \frac{27}{8}(11+2\epsilon)^2\alpha_y\alpha_g^3 + \frac{1}{4}(20+3\epsilon)(11+2\epsilon)^2\alpha_y^2\alpha_g^2,\\
\beta_g^{(4)} &= -\left[\frac{14731}{72}+550\zeta_3+\left(\frac{123473}{324}+\frac{1808}{9}\zeta_3\right)\epsilon+\left(\frac{21598}{243}+\frac{56}{3}\zeta_3\right)\epsilon^2+\frac{260}{243}\epsilon^3\right]\alpha_g^5\\
&\quad+\frac{1}{48}(11+2\epsilon)^2\left[\left(-107+432\zeta_3+\frac{758}{3}\epsilon\right)\alpha_y\alpha_g^4+3(647-48\zeta_3+92\epsilon)\alpha_y^2\alpha_g^3\right]\\
&\quad+(11+2\epsilon)^2\left[3\alpha_u^2-\left(\frac{875}{16}+\frac{179}{12}\epsilon+\frac{11}{12}\epsilon^2\right)\alpha_y^2\right]\alpha_y\alpha_g^2-\frac{5}{4}(11+2\epsilon)^3\alpha_u\alpha_y^2\alpha_g^2.
\end{aligned} \tag{14}$$

We note that irrational coefficients $\propto \zeta_3$ arise for the first time at four-loop. Further, the quartic coupling α_u makes its first appearance at four-loop, as it must.[5] This influence of the scalar sector is channeled through the Yukawa sector, which itself is supplemented by three-loop results

$$\begin{aligned}
\beta_y^{(1)} &= (13+2\epsilon)\alpha_y^2 - 6\alpha_g\alpha_y,\\
\beta_y^{(2)} &= -\frac{1}{8}(35+2\epsilon)(11+2\epsilon)\alpha_y^3 + (49+8\epsilon)\alpha_g\alpha_y^2 - 4(11+2\epsilon)\alpha_u\alpha_y^2 - \frac{1}{6}(93-20\epsilon)\alpha_g^2\alpha_y + 4\alpha_u^2\alpha_y,\\
\beta_y^{(3)} &= \left(\frac{17413}{64}+\frac{2595}{32}\epsilon+\frac{59}{16}\epsilon^2-\frac{3}{8}\epsilon^3\right)\alpha_y^4 - \frac{1}{2}(118+19\epsilon)(11+2\epsilon)\alpha_g\alpha_y^3 + 6(8+\epsilon)(11+2\epsilon)\alpha_u\alpha_y^3\\
&\quad-\left[\frac{1217}{16}+198\zeta_3+\frac{1}{8}\epsilon(893+288\zeta_3+136\epsilon)\right]\alpha_g^2\alpha_y^2 + 2(11+2\epsilon)\alpha_g\alpha_u\alpha_y^2 + 5\left(\frac{5}{2}+\epsilon\right)\alpha_u^2\alpha_y^2 - 8\alpha_u^3\alpha_y\\
&\quad+\left[\frac{641}{6}+132\zeta_3+\frac{\epsilon}{27}(1947+648\zeta_3+70\epsilon)\right]\alpha_g^3\alpha_y.
\end{aligned} \tag{15}$$

In the quartic sector, the gauge dependent terms $\propto \alpha_g$ and $\propto \alpha_g^2$ are computed here for the first time. These terms must vanish for $\alpha_y = 0$, which decouples the fermionic from the gauge sector. This is indeed manifest in the evolution of both the single- and double-trace quartics. The latter reads

[5]Had the scalars been charged under the gauge symmetry, contributions would have appeared at three-loop.

$$
\begin{aligned}
\beta_u^{(1)} &= 8\alpha_u^2 + 4\alpha_y\alpha_u - (11+2\epsilon)\alpha_y^2,\\
\beta_u^{(2)} &= -24\alpha_u^3 - 16\alpha_y\alpha_u^2 - 3(11+2\epsilon)\alpha_y^2\alpha_u + 10\alpha_g\alpha_y\alpha_u + (11+2\epsilon)^2\alpha_y^3 - 2(11+2\epsilon)\alpha_g\alpha_y^2,\\
\beta_u^{(3)} &= 104\alpha_u^4 + 34\alpha_u^3\alpha_y + (889+166\epsilon)\alpha_u^2\alpha_y^2 - \frac{1}{8}\left(\frac{11}{2}+\epsilon\right)^2(21-26\epsilon)\alpha_y^4 - \left(\frac{2953}{16}+\frac{315}{8}\epsilon\right)(11+2\epsilon)\alpha_u\alpha_y^3\\
&\quad - (102-96\zeta_3)\alpha_u^2\alpha_y\alpha_g + \frac{1}{4}(11+2\epsilon)(149-240\zeta_3)\alpha_u\alpha_y^2\alpha_g - \frac{1}{4}(11+2\epsilon)^2(5-24\zeta_3)\alpha_y^3\alpha_g\\
&\quad + \left(\frac{13}{4}-8\epsilon\right)\alpha_u\alpha_y\alpha_g^2 + \frac{1}{8}(11+2\epsilon)(23+20\epsilon)\alpha_y^2\alpha_g^2.
\end{aligned}
\tag{16}
$$

Note the absence of a term $\propto \alpha_y\alpha_g^3$, which can easily be understood diagrammatically. As expected in the planar large-N limit [95], the double-trace quartic does not enter other β functions than its own, namely

$$
\begin{aligned}
\beta_v^{(1)} &= 12\alpha_u^2 + 16\alpha_u\alpha_v + 4\alpha_v^2 + 4\alpha_y\alpha_v,\\
\beta_v^{(2)} &= -96\alpha_u^3 - 40\alpha_u^2\alpha_v - 24\alpha_y\alpha_u^2 - 32\alpha_y\alpha_u\alpha_v - 8\alpha_y\alpha_v^2 + 4(11+2\epsilon)\alpha_u\alpha_y^2 - 3(11+2\epsilon)\alpha_v\alpha_y^2 + 10\alpha_g\alpha_y\alpha_v + (11+2\epsilon)^2\alpha_y^3,\\
\beta_v^{(3)} &= 12\alpha_v^2\alpha_u^2 + 480\alpha_v\alpha_u^3 + (772+384\zeta_3)\alpha_u^4 + 66\alpha_v\alpha_u^2\alpha_y + 192\alpha_u^3\alpha_y + \left(\frac{427}{2}+41\epsilon\right)\alpha_v^2\alpha_y^2\\
&\quad + \left(788+152\epsilon+96\zeta_3\left(\frac{11}{2}+\epsilon\right)\right)\alpha_v\alpha_u\alpha_y^2 + \left(\frac{1985}{2}+187\epsilon+192\zeta_3\left(\frac{11}{2}+\epsilon\right)\right)\alpha_u^2\alpha_y^2 - 4\left(\frac{11}{2}+\epsilon\right)\\
&\quad \times\left(105+22\epsilon+24\zeta_3\left(\frac{11}{2}+\epsilon\right)\right)\alpha_u\alpha_y^3 - \frac{1}{8}\left(\frac{11}{2}+\epsilon\right)(1545+374\epsilon)\alpha_v\alpha_y^3 - \left(\frac{11}{2}+\epsilon\right)^2(73+10\epsilon)\alpha_y^4\\
&\quad - 9(17-16\zeta_3)\alpha_u^2\alpha_y\alpha_g - (204-192\zeta_3)\alpha_v\alpha_u\alpha_y\alpha_g - (51-48\zeta_3)\alpha_v^2\alpha_y\alpha_g + 8(11+2\epsilon)(7-9\zeta_3)\alpha_u\alpha_y^2\alpha_g\\
&\quad + \frac{1}{4}(11+2\epsilon)(149-240\zeta_3)\alpha_v\alpha_y^2\alpha_g + \frac{1}{2}(11+2\epsilon)^2(-1+12\zeta_3)\alpha_y^3\alpha_g + \left(\frac{13}{4}-8\epsilon\right)\alpha_v\alpha_y\alpha_g^2 + 6(11+2\epsilon)^2\alpha_y^2\alpha_g^2,
\end{aligned}
\tag{17}
$$

where it only appears to order $\propto \alpha_v^2$. This potentially leads to pair-wise fixed-point solutions that only differ by α_v^* and potentially merge at some value of ϵ, disappearing into the complex plane. Finite-N corrections to (14)–(17) are more lengthy and can be found in Appendix B.

B. Anomalous dimensions

Next, we provide some results for physical meaningful anomalous dimensions for mass and field strength renormalization. The scalar squared mass m^2 in (1) corresponds to the only bilinear field operator that does not violate local or global symmetries. Its gauge-independent anomalous dimension

$$
\gamma_{m^2} = \frac{\mathrm{d}\ln m^2}{\mathrm{d}\ln\mu} = \sum_{\ell=1}^{\infty}\gamma_{m^2}^{(\ell)} \tag{18}
$$

cannot be obtained from our loop computation, since we have chosen $m^2 = 0$ for convenience. Thus, its counterterm is tainted by contributions from the gauge boson IRA mass. Instead, we make use of the general β functions for the quartic interactions and employ the dummy field trick [49,76,96] to obtain mass β functions. At three-loops, we rely on the ansatz detailed in Appendix A of tensor structures with the incomplete set of coefficients extracted from the literature (see Sec. III). The information is sufficient to obtain

$$
\begin{aligned}
\gamma_{m^2}^{(1)} &= 8\alpha_u + 4\alpha_v + 2\alpha_y,\\
\gamma_{m^2}^{(2)} &= -20\alpha_u^2 - 8\alpha_v\alpha_y - 16\alpha_u\alpha_y + 5\alpha_y\alpha_g - \frac{3}{2}(11+2\epsilon)\alpha_y^2,\\
\gamma_{m^2}^{(3)} &= 240\alpha_u^3 + 12\alpha_v\alpha_u^2 + 33\alpha_u^2\alpha_y + \frac{1}{2}(427+82\epsilon)\alpha_v\alpha_y^2 + (394+264\zeta_3+76\epsilon+48\zeta_3\epsilon)\alpha_u\alpha_y^2 + 3(16\zeta_3-17)\\
&\quad \times(2\alpha_u+\alpha_v)\alpha_y\alpha_g - \frac{1}{32}(11+2\epsilon)(1545+374\epsilon)\alpha_y^3 - \frac{1}{8}(11+2\epsilon)(240\zeta_3-149)\alpha_y^2\alpha_g + \frac{1}{8}(13-32\epsilon)\alpha_y\alpha_g^2,
\end{aligned}
\tag{19}
$$

while anomalous dimensions of other scalar bilinear operators violating global symmetries cannot be determined.

As for the fermions, a Dirac mass term $m_\psi\overline{\psi}\psi$ breaks the global symmetry but leaves the gauge symmetry intact. Its anomalous dimension can be extracted from the generic Yukawa β function up to three-loops [40,41], again using the dummy field trick. Employing the notation

$$\gamma_{m_\psi} = \frac{\mathrm{d}\ln m_\psi}{\mathrm{d}\ln\mu} = \sum_{\ell=1}^{\infty}\gamma_{m_\psi}^{(\ell)}, \tag{20}$$

the results read

$$\begin{aligned}
\gamma_{m_\psi}^{(1)} &= \frac{1}{2}(11+2\epsilon)\alpha_y - 3\alpha_g,\\
\gamma_{m_\psi}^{(2)} &= -\frac{1}{16}(11+2\epsilon)(23+2\epsilon)\alpha_y^2 + 2(11+2\epsilon)\alpha_y\alpha_g - \frac{1}{12}(93-20\epsilon)\alpha_g^2,\\
\gamma_{m_\psi}^{(3)} &= -\frac{11}{4}(11+2\epsilon)\alpha_u^2\alpha_y + (11+2\epsilon)^2\alpha_u\alpha_y^2 + \left(\frac{13387}{128} + \frac{2119}{64}\epsilon + \frac{49}{32}\epsilon^2 - \frac{3}{16}\epsilon^3\right)\alpha_y^3\\
&\quad - \frac{1}{8}(11+2\epsilon)(477-48\zeta_3+76\epsilon)\alpha_y^2\alpha_g - \frac{1}{16}(11+2\epsilon)(113+288\zeta_3+136\epsilon)\alpha_y\alpha_g^2\\
&\quad + \left(\frac{641}{12} + 66\zeta_3 + \frac{649}{18}\epsilon + 12\zeta_3\epsilon + \frac{35}{27}\epsilon^2\right)\alpha_g^3.
\end{aligned} \tag{21}$$

Furthermore, a renormalization procedure of all field X has been conducted via the substitution

$$X_{\mathrm{bare}} = \sqrt{Z_X}X. \tag{22}$$

These field strength renormalization factors Z_X contain counterterms and imply anomalous dimensions

$$\gamma_X = \frac{\mathrm{d}\ln\sqrt{Z_X}}{\mathrm{d}\ln\mu} = \sum_{\ell=1}^{\infty}\gamma_X^{(\ell)}. \tag{23}$$

Note that all factors Z_X are just multiplicative numbers as the global symmetries remain intact. This excludes any ambiguities stemming from anti-Hermitian parts of anomalous dimension matrices [68–71]. However, field strength anomalous dimensions γ_X are in general gauge dependent and thus unphysical. The scalar field anomalous dimension γ_ϕ represents a notable exception, as its fixed point value is part of the CFT data. Unsurprisingly, we find it to be gauge independent up to three-loop order

$$\begin{aligned}
\gamma_\phi^{(1)} &= \alpha_y,\\
\gamma_\phi^{(2)} &= 2\alpha_u^2 + \frac{5}{2}\alpha_y\alpha_g - \frac{3}{4}(11+2\epsilon)\alpha_y^2,\\
\gamma_\phi^{(3)} &= -4\alpha_u^3 - \frac{15}{2}\alpha_u^2\alpha_y + \frac{5}{2}(11+2\epsilon)\alpha_u\alpha_y^2 + \frac{1}{64}(183+10\epsilon)(11+2\epsilon)\alpha_y^3 - \frac{1}{16}(48\zeta_3-5)(11+2\epsilon)\alpha_y^2\alpha_g\\
&\quad + \frac{1}{16}(13-32\epsilon)\alpha_y\alpha_g^2.
\end{aligned} \tag{24}$$

As for the other fields, anomalous dimensions in R_ξ gauge are collected in Appendix C.

C. Fixed point

With beta functions available at the complete 433 order, we are now in a position to determine interacting fixed points accurately up to complete cubic order in the Veneziano parameter ϵ. Complete sets of coefficients up to quadratic order have previously been found in [8] (see also [3]).

Using the expansion (7), and solving $\beta_i(\alpha_j^*) = 0$ systematically as a power series in ϵ, we find for the gauge coupling coefficients

$$\alpha_g^{(1)} = \frac{26}{57},$$
$$\alpha_g^{(2)} = 23\frac{75245 - 13068\sqrt{23}}{370386},$$
$$\alpha_g^{(3)} = \frac{353747709269}{2406768228} - \frac{663922754}{22284891}\sqrt{23} + \frac{386672}{185193}\zeta_3. \tag{25}$$

Note that ζ_3 arises for the first time in the cubic coefficient. Similarly, for the Yukawa coupling we obtain

$$\alpha_y^{(1)} = \frac{4}{19},$$
$$\alpha_y^{(2)} = \frac{43549}{20577} - \frac{2300}{6859}\sqrt{23},$$
$$\alpha_y^{(3)} = \frac{2893213181}{44569782} - \frac{96807908}{7428297}\sqrt{23} + \frac{4576}{6859}\zeta_3. \tag{26}$$

The single- and double-trace quartic scalar couplings give rise to the coefficients

$$\alpha_u^{(1)} = \frac{\sqrt{23} - 1}{19},$$
$$\alpha_u^{(2)} = \frac{365825\sqrt{23} - 1476577}{631028},$$
$$\alpha_u^{(3)} = -\frac{5173524931447\sqrt{23} - 24197965967251}{282928976136} - \frac{416(\sqrt{23} - 12)}{6859}\zeta_3 \tag{27}$$

and

$$\alpha_v^{(1)} = \frac{\sqrt{20 + 6\sqrt{23}} - 2\sqrt{23}}{19},$$
$$\alpha_v^{(2)} = \frac{-643330\sqrt{23} + 2506816}{631028} + \frac{452563\sqrt{23} - 1542518}{315514\sqrt{20 + 6\sqrt{23}}},$$
$$\alpha_v^{(3)} = \frac{442552351896048 - 249223363466258\sqrt{23}}{282928976136(307 + 60\sqrt{23})} + \frac{(122834160737083 - 26761631049822\sqrt{23})\sqrt{20 + 6\sqrt{23}}}{282928976136(307 + 60\sqrt{23})}$$
$$+ \frac{659988864\zeta_3(942 - 338\sqrt{23} + 39\sqrt{2(-529426 + 583581\sqrt{23})})}{282928976136(307 + 60\sqrt{23})}, \tag{28}$$

respectively. Numerically, the expansions read

$$\alpha_g^* = 0.456\epsilon + 0.781\epsilon^2 + 6.610\epsilon^3 + 24.137\epsilon^4,$$
$$\alpha_y^* = 0.211\epsilon + 0.508\epsilon^2 + 3.322\epsilon^3 + 15.212\epsilon^4,$$
$$\alpha_u^* = 0.200\epsilon + 0.440\epsilon^2 + 2.693\epsilon^3 + 12.119\epsilon^4,$$
$$\alpha_v^* = -0.137\epsilon - 0.632\epsilon^2 - 4.313\epsilon^3 - 24.147\epsilon^4, \tag{29}$$

where we have neglected subleading corrections $\propto \epsilon^5$. All coefficients up to and including $\propto \epsilon^3$ remain unchanged even if higher loops are included. To indicate the trend beyond the strict 433 approximation, we also show the incomplete next-order coefficients $\propto \epsilon^4$ that will receive as-of-yet unknown corrections at order 544. At the preceding loop order 322, for example, the incomplete contributions $\propto \epsilon^3$ accounted for 60%–85% of the complete cubic coefficients at order 433 [8]. We note from (29) that corrections for all couplings at any order arise with the same sign, and that the cubic coefficients are almost an order of magnitude larger than the quadratic ones.

Finally, we note that since β_v is quadratic in α_v to any loop order in perturbation theory [95], there also exists a second fixed point solution in the double-trace sector with $\alpha_{v-}^* \leq \alpha_v^*$ and the coordinates for $\alpha_{g,y,u}^*$ unchanged [3,17]. This second solution, however, is unphysical in that it leads to an unstable vacuum [3,17].

D. Scaling exponents

Universal critical exponents are obtained as the eigenvalues of the stability matrix

$$M_{ij} = \left.\frac{\partial\beta_i}{\partial\alpha_j}\right|_{\alpha=\alpha^*} \tag{30}$$

and can equally be expanded as a power series in the Veneziano parameter,

$$\vartheta_i = \sum_{n=1}^{\infty} \epsilon^n \vartheta_i^{(n)}. \tag{31}$$

The stability matrix factorizes because the double-trace coupling does not couple back into the single-trace couplings in the Veneziano limit. Quantitatively, we then find a single relevant and three irrelevant eigenvalues,

$$\vartheta_1 < 0 < \vartheta_2 < \vartheta_3 < \vartheta_4, \tag{32}$$

and the UV critical surface due to canonically marginal interactions is one dimensional, with ϑ_3 the isolated eigenvalue for the double-trace quartic.

For ϑ_1, the expansion starts out at quadratic order and is accurate up to and including the fourth order,

$$\begin{aligned}
\vartheta_1^{(1)} &= 0,\\
\vartheta_1^{(2)} &= -\frac{104}{171},\\
\vartheta_1^{(3)} &= \frac{2296}{3249},\\
\vartheta_1^{(4)} &= \frac{1405590649319}{15643993482} - \frac{15630102884}{869110749}\sqrt{23}\\
&\quad + \frac{1546688}{555579}\zeta_3.
\end{aligned} \tag{33}$$

The irrelevant directions start out at linear order and are accurate up to the cubic order in ϵ. We find

$$\begin{aligned}
\vartheta_2^{(1)} &= \frac{52}{19},\\
\vartheta_2^{(2)} &= \frac{136601719 - 22783308\sqrt{23}}{4094823},\\
\vartheta_2^{(3)} &= -\frac{119064152144668585}{117078859819806} + \frac{93098590593718400}{448802295975923}\sqrt{23},
\end{aligned} \tag{34}$$

as well as

$$\begin{aligned}
\vartheta_3^{(1)} &= \frac{8}{19}\sqrt{20+6\sqrt{23}},\\
\vartheta_3^{(2)} &= \frac{4(-1682358+410611\sqrt{23})}{157757\sqrt{20+6\sqrt{23}}},\\
\vartheta_3^{(3)} &= 2\frac{96845792758245\sqrt{23}+8579855232(19847+6564\sqrt{23})\zeta_3}{35366122017(307+60\sqrt{23})\sqrt{20+6\sqrt{23}}} - 2\frac{616512472540856}{35366122017(307+60\sqrt{23})\sqrt{20+6\sqrt{23}}},
\end{aligned} \tag{35}$$

and finally

$$\begin{aligned}
\vartheta_4^{(1)} &= \frac{16}{19}\sqrt{23},\\
\vartheta_4^{(2)} &= -\frac{44492672}{1364941} + \frac{272993948}{31393643}\sqrt{23},\\
\vartheta_4^{(3)} &= \frac{2(-174067504271892880236+37418532792608300581\sqrt{23})}{278706225801048183}.
\end{aligned} \tag{36}$$

Numerically, the expansion coefficients read

$$\begin{aligned}
\vartheta_1 &= -0.608\epsilon^2 + 0.707\epsilon^3 + 6.947\epsilon^4 + 4.825\epsilon^5,\\
\vartheta_2 &= 2.737\epsilon + 6.676\epsilon^2 + 22.120\epsilon^3 + 102.55\epsilon^4,\\
\vartheta_3 &= 2.941\epsilon + 1.041\epsilon^2 + 5.137\epsilon^3 - 62.340\epsilon^4,\\
\vartheta_4 &= 4.039\epsilon + 9.107\epsilon^2 + 38.646\epsilon^3 + 87.016\epsilon^4,
\end{aligned} \tag{37}$$

up to subleading corrections in ϵ. We recall that all coefficients up to order ϵ^4 for ϑ_1 and up to order ϵ^3 for $\vartheta_{2,3,4}$ remain unchanged even if higher loops are included, and that the new coefficients from the order 433 are about $\mathcal{O}(4\text{–}9)$ times larger than those from the preceding order 322. Once more, to indicate the trend beyond 433, we also show the incomplete next-order coefficient.

E. Bounds from series expansions

Next, we exploit the expansions of fixed point couplings and exponents to estimate the size of the conformal window $\epsilon \leq \epsilon_{\max}$, focusing on the coefficients that are unambiguously determined up to order 433.

To satisfy vacuum stability, the quartic couplings must obey the conditions $0 \leq \alpha_u$ and $0 \leq \alpha_w \equiv \alpha_u + \alpha_v$ [17,97]. The former is always satisfied, as can be seen from (29). Using the exact fixed point couplings for the latter, we find the series expansion

$$\alpha_w^* = 0.063\epsilon - 0.192\epsilon^2 - 1.620\epsilon^3 + \mathcal{O}(\epsilon^4). \quad (38)$$

Corrections arise with a sign opposite to the leading term. At order ϵ^2, this implies $\epsilon \leq \epsilon_{\max}$, with $\epsilon_{\max} \approx 0.327$ [8,13]. At order ϵ^3, the bound tightens by more than a factor of 2, $\epsilon_{\max} \approx 0.147$. As an estimate for higher order corrections in ϵ, we also employ a Padé resummation by writing (38) as $\alpha_w^* = \frac{A\epsilon + B\epsilon^2}{1+C\epsilon}$ (and similarly for other couplings).[6] Using the Padé approximant suggests that higher order effects tighten the constraint even further, $\epsilon_{\max} \approx 0.087$. Overall, we conclude that the series expansion (38) indicates a loss of vacuum stability in the range

$$\epsilon_{\max} \approx 0.087\text{–}0.146. \quad (39)$$

We now turn to the expansion of scaling exponents, Eq. (37). From the explicit expressions up to order 433, we notice that the series expansion for exponents ϑ_2, ϑ_3, and ϑ_4 are monotonous, with same-sign corrections to the leading order, at every order. However, the relevant scaling exponent ϑ_1 has all higher-order contributions with a sign opposite to the leading one. An overall change of sign is indicative for a collision of the UV fixed point with an IR fixed point. We estimate $\epsilon_{\max}$ from solving $\vartheta_1 = 0$ and reproduce the result $\epsilon_{\max} \approx 0.860$ at order ϵ^3 [8,13]. The newly established coefficient at order ϵ^4 now tightens the constraint by roughly a factor of 3, $\epsilon_{\max} \approx 0.249$. Using a Padé approximant as before, we find an even tighter estimate $\epsilon_{\max} \approx 0.091$. Overall, the series expansion indicates that the conformal window terminates due to a fixed point merger in the range

$$\epsilon_{\max} \approx 0.091\text{–}0.249. \quad (40)$$

Next, we ask whether the fixed point can disappear due to a merger in the double-trace sector, $\alpha_{v-}^* \to \alpha_v^*$ [98]. If so, it implies a double-zero of β_v and the corresponding scaling exponent must vanish, $\vartheta_3 = 0$. However, the first three universal expansion coefficients have all the same sign, Eq. (37), giving no hints for a zero at 433. Also, computing the difference between the double-trace quartic couplings $\Delta\alpha_v \equiv \alpha_v^* - \alpha_{v-}^*$ we find

$$\Delta\alpha_v^* = 0.735\epsilon + 0.570\epsilon^2 + 0.326\epsilon^3 + \mathcal{O}(\epsilon^4). \quad (41)$$

The first three expansion coefficients in (41) have all the same sign, offering no hints for a zero for any $\epsilon > 0$. We conclude that a merger in the double-trace sector is not supported by the 433 data.

Finally, we provide a rough estimate for the range in ϵ with perturbative control. Based on naive dimensional analysis with couplings scaled in units of natural loop factors [99], as done here, we take the view that this regime is characterized by $0 < |\alpha^*| \lesssim 1$.[7] We note that the expansion coefficients (29) of the single- (double-) trace couplings receive only positive (negative) contributions, implying $\alpha_{g,y,u}^* > 0$ and $\alpha_v^* < 0$, and that the tightest bound $\epsilon < \epsilon_{\text{strong}}$ arises from the gauge coupling. We find $\epsilon_{\text{strong}} \approx 0.877$ at order ϵ^2, and $\epsilon_{\text{strong}} \approx 0.457$ at order ϵ^3. To estimate higher order effects in ϵ, we once more use a Padé approximant for the gauge coupling fixed point and find the tighter bound $\epsilon_{\text{strong}} \approx 0.117$, suggesting an onset of strong coupling in the range

$$\epsilon_{\text{strong}} \approx 0.117\text{–}0.457. \quad (42)$$

We notice that regimes with vacuum instability or a fixed point merger are reached before the theory becomes strongly coupled. Also, in all cases (39), (40), (42), the tightest parameter bound arises from the Padé resummations, giving bounds of the same size as obtained from the 322 beta functions [8].

In summary, the constraints on the conformal window as derived from series expansions of couplings have become tighter, owing to the corrections established at order 433 over those at order 322. The overall picture shows that

$$\epsilon_{\max} < \epsilon_{\text{strong}} \quad (43)$$

for each of the successive approximation orders 322, 433, and for a Padé approximant of the latter. Results also indicate that the conformal window is primarily limited by the onset of vacuum instability and a nearby fixed point merger, rather than a merger in the double-trace sector or the onset of strong coupling. Our results are further illustrated in Fig. 4, including an extrapolation to finite field multiplicities (N_c, N_f). In particular, the smallest set of integer multiplicities compatible with an interacting UV fixed point increases from $(N_c, N_f)|_{\min} = (3, 17)$ at order 322 to $(N_c, N_f)|_{\min} = (5, 28)$ at order 433, and to $(N_c, N_f)|_{\min} = (7, 39)$ if we were to consider the forecast

[6]Notice that the loop order 433 is the first perturbative order where resummation techniques can be applied.

[7]We stress that this criterion is not rigorous and must be confirmed with higher loops or nonperturbatively.

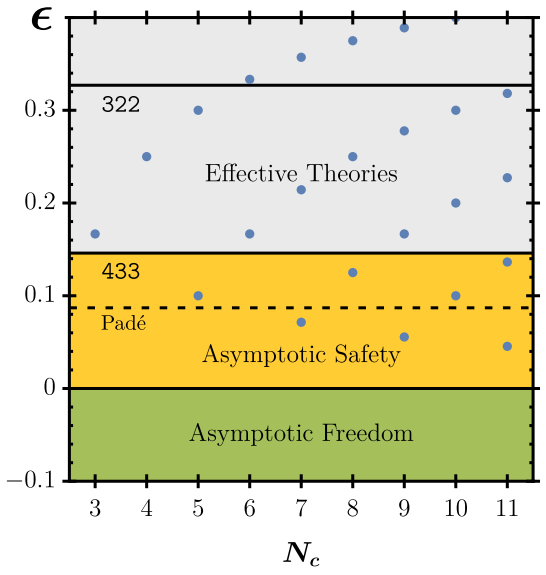

FIG. 4. The size of the UV conformal window (yellow band) from series expansions, comparing the new upper bound on ϵ at order 433 and the Padé approximant bound (dashed line) [see (39)] with the previous upper bounds at order 322 [8]. Also shown are regimes with asymptotic freedom (green) and effective theories (gray). Dots indicate integer values for (N_c, N_f) in the (ϵ, N_c) plane.

from Padé approximants. We defer a more detailed investigation of the conformal window to a forthcoming publication [100].

F. Unitarity

In our setting, scale invariance at the weakly interacting UV fixed point entails full conformal invariance [101], and the critical theory can be described by a CFT. Accordingly, the bound on unitarity for a spin-0 operator $\mathcal{O}$

$$\Delta_{\mathcal{O}} = \dim \mathcal{O} + \gamma^*_{\mathcal{O}} \geq 1 \tag{44}$$

must be observed [102]. These CFT constraints can be addressed by exploiting our results for anomalous dimensions (19)–(24) and fixed points (29). We find

$$\begin{aligned}
\gamma^*_{\phi} &= 0.2105\epsilon + 0.4625\epsilon^2 + 2.471\epsilon^3 + \mathcal{O}(\epsilon^4),\\
\gamma^*_{m^2} &= 1.470\epsilon + 0.5207\epsilon^2 + 2.568\epsilon^3 + \mathcal{O}(\epsilon^4),\\
\gamma^*_{m_\psi} &= -0.2105\epsilon + 0.4628\epsilon^2 + 0.3669\epsilon^3 + \mathcal{O}(\epsilon^4),
\end{aligned} \tag{45}$$

retaining all terms determined unambiguously in the ϵ expansion at 433. Subleading terms starting at order ϵ^4 necessitate the full 544 approximation.

We observe from (45) that the scalar field and mass anomalous dimensions γ^*_{ϕ} and $\gamma^*_{m^2}$ are manifestly positive and satisfy (44) without further ado. On the other hand, the fermion mass anomalous dimension $\gamma^*_{m_\psi}$ comes out negative to the leading order. Still, the subleading positive contributions up to cubic order in ϵ ensure that the anomalous dimension remains strictly bounded from below, $\gamma^*_{m_\psi} \gtrsim -0.02$. In consequence, it cannot become sufficiently negative for $\Delta_{\bar\psi\psi}$ to fall below the unitarity bound (44). Altogether, we conclude that the unitarity constraints (44) are satisfied nonmarginally in perturbation theory. Moreover, unitarity does not offer bounds on ϵ within the conformal window.

G. Scales and phase diagram

We are now in a position to revisit the phase diagram of the theory. Figure 1 illustrates the phase diagram in the 433 approximation. Trajectories are shown in the (α_g, α_y) plane, with arrows pointing from the UV to the IR. Evidently, asymptotic freedom is absent and the Gaussian fixed point is an IR attractive fixed point for all couplings. Nevertheless, the theory is UV complete and remains predictive up to the highest energies, courtesy of the interacting UV fixed point. It displays a single relevant direction among the classically marginal interactions. Without loss of generality, we take

$$\delta\alpha_g = \alpha_g - \alpha^*_g \tag{46}$$

as the fundamentally free parameter at the high scale μ_0. The running of the Yukawa and quartic couplings $\alpha_i(\mu)$ with $i = y, u, v$ is entirely dictated by the running of $\alpha_g(\mu)$, and they can be expressed in terms of the gauge coupling as $\alpha_i(\mu) = F_i[\alpha_g(\mu)]$ for suitable functions F_i. The IR fate of trajectories emanating from the fixed point is determined by whether $\delta\alpha_g < 0$ or $\delta\alpha_g > 0$ at the high scale. In the former case, the theory becomes free in the infrared. In the latter case, the theory becomes strongly coupled and displays either confinement (such as in QCD) or IR conformality such as at an interacting IR fixed point. Our results are illustrated in Fig. 5, where sample trajectories connecting the UV fixed point with the IR are shown, also contrasting settings for initial conditions $\delta\alpha_g(\mu_0) < 0$ (left panel) leading to IR freedom, with initial conditions $\delta\alpha_g(\mu_0) > 0$ (right panel).

The transition from the UV to the IR is characterized by an RG-invariant scale Λ_c, analogous to $\Lambda_{\rm QCD}$ in QCD. It arises through dimensional transmutation from the dimensionless fundamental parameter $\delta\alpha_g \ll |\alpha^*_g|$ at the high scale μ, and reads

$$\Lambda_c \propto \mu \cdot |\delta\alpha(\mu)|^{\nu}, \tag{47}$$

where $\nu = -1/\vartheta_1$ with ϑ_1 the relevant scaling exponent (37). One readily confirms that $\mathrm{d}\Lambda_c/\mathrm{d}\ln\mu = 0$. The proportionality constant c can be determined from a crossover condition. For $\delta\alpha_g > 0$, strong coupling sets in as soon as $\delta\alpha_g$ is of order unity; hence $c \approx 1$. For negative $\delta\alpha_g$, the

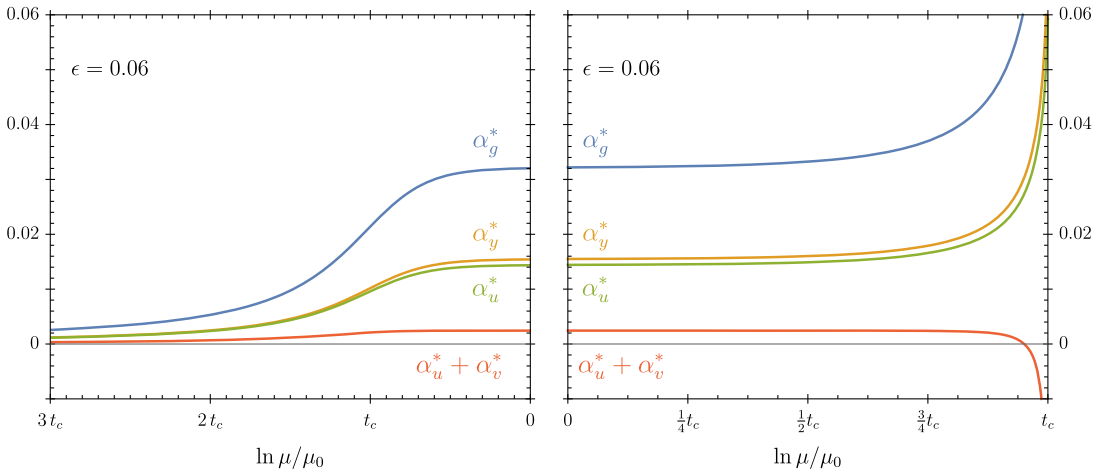

FIG. 5. Running couplings along UV-IR connecting trajectories emanating out of the interacting UV fixed point, corresponding to the (orange) separatrices highlighted in Fig. 1. Trajectories with UV initial condition $\delta\alpha_g(\mu_0) < 0$ approach a free theory in the IR (left panel), while those with $\delta\alpha_g(\mu_0) > 0$ enter a strongly coupled regime with either confinement or conformality in the IR (right panel). Here, $t_c = \ln \Lambda_c/\mu_0$ with Λ_c as in (47) and (49), respectively, and $\epsilon = 0.06$.

Gaussian fixed point takes over as soon as $\delta\alpha_g \approx -\alpha_g^*/3$ [17], giving $c = (3/\alpha_*)^\nu$ instead.

We briefly compare this with asymptotically free theories by taking $\epsilon < 0$. In this case, the UV critical surface is now two-dimensional with both the gauge and the Yukawa coupling being marginally relevant. We then find a range of asymptotically free trajectories emanating from the Gaussian fixed point and characterized by

$$\delta\alpha_g = \alpha_g - \alpha_g^*,$$
$$\delta\alpha_y = \alpha_y - \alpha_y^*. \tag{48}$$

For sufficiently small $0 < -\epsilon \ll 1$ and $\alpha_y = 0$, the theory also displays a Banks-Zaks fixed point α_g^* of order $|\epsilon|$ and $\alpha_i^* = 0 (i = y, u, v)$. In either case, we find the transition scale Λ_c as

$$\Lambda_c \propto \mu \cdot \exp\left(\frac{1}{\beta_g^{(1)} \delta\alpha(\mu)}\right), \tag{49}$$

characteristic for asymptotic freedom, with a negative one-loop gauge coefficient $\beta_g^{(1)} < 0$. All trajectories run toward strong coupling where either confinement or conformality take over, except for the trajectory that terminates at the Banks-Zaks fixed point.

Even though the UV critical surface is two-dimensional, it is interesting to note that the Yukawa nullcline is an IR attractor and all outgoing trajectories collapse onto it. Hence, as soon as the gauge coupling becomes of the order of the one-loop gauge coefficient, $\alpha(\mu) \gtrsim |\epsilon|$, outgoing trajectories along the nullcline of the asymptotically free theory (with $0 < -\epsilon \ll 1$) become indistinguishable from the outgoing trajectory of the asymptotically safe theory (with $0 < \epsilon \ll 1$).

V. DISCUSSION AND OUTLOOK

The quantum field theory (1) provides an important template for an asymptotically safe 4D particle theory with an interacting and perturbatively controlled fixed point at highest energies. We have extended the investigation of the UV theory up to four-loops in perturbation theory, a prerequisite to achieve the complete cubic order in the underlying conformal expansion in terms of a small Veneziano parameter ϵ. The central input for this is the four-loop gauge, three-loop Yukawa and quartic β functions, and three-loop anomalous dimensions. We have computed the previously missing pieces that are the three-loop contributions to scalar β functions containing gauge interactions (Sec. III).

With these results at hand, we have determined all fixed point couplings, critical exponents, and anomalous dimensions up to the third nontrivial order in ϵ, also investigating the phase diagram and UV-IR connecting trajectories (Sec. IV). Findings are in accord with unitarity, as they must. Most notably, bounds on the conformal window of (39) and (40) have become tighter in comparison with the preceding order, and they strengthen the view that the upper boundary remains under perturbative control. Our work further substantiates the existence of the fixed point at finite values of the Veneziano parameter and at finite N. Ultimately, conformality is lost due to the onset of vacuum instability and a nearby fixed point merger, Eq. (43), rather than through a merger in the double-trace sector or strong coupling phenomena.

While our results have been achieved specifically for Dirac fermions coupled to SU gauge fields and complex scalars ϕ_{ij} (see Table I), they equally hold true for theories with Majorana fermions coupled to either SO gauge fields with symmetric complex scalars $\phi_{(ij)}$ or to Sp gauge fields

with antisymmetric scalars $\phi_{[ij]}$ [11]. The reason for this is that these three types of matter-gauge theories are mutually equivalent to each other in the Veneziano limit, even though field content, gauge symmetries, and global symmetries are different [11]. In particular, and modulo the normalization of couplings, their beta functions are identical to any loop order, and results of this work are equally valid for the partner theories.

We close with a few comments from the viewpoints of lattice Monte Carlo simulations, conformal field theory, and model building. It would be valuable to explore the UV conformal window using complementary tools such as the lattice, taking advantage of the vast body of works on IR fixed points in 4D matter-gauge theories [103]. In a related vein, in our QFT setting, scale invariance at the UV fixed point entails full conformal invariance [101]. Hence, our renormalization group results offer direct access to conformal data characterizing an interacting 4D CFT [104,105]. It would then be equally important to investigate the 4D UV critical theory using first-principle CFT methods such as the bootstrap [106], or other. Finally, we emphasize that our setting provides a blueprint for concrete 4D nonsupersymmetric CFTs with standard model-like field content in the UV, which invites further model building.

ACKNOWLEDGMENTS

We are thankful to Anders Eller Thomsen for comments about parametrizing γ_5 diagrams. Some of our results have been presented by one of us (T. S.) at *Asymptotic Safety Meets Particle Physics IX*, Dec. 2022, DESY, Hamburg, and at *Loopfest XXI*, June 2023, SLAC National Accelerator Laboratory. This work is supported by the Science and Technology Facilities Council (STFC) under the Consolidated Grant No. ST/T00102X/1 (D. L.).

APPENDIX A: TENSOR STRUCTURES FOR THREE-LOOP QUARTIC RGES

In this appendix, we detail the general structure for three-loop scalar field anomalous dimensions and quartic β functions of any renormalizable QFT with uncharged scalars. We closely follow the notation of [53] with the Lagrangian

$$\begin{aligned}\mathcal{L} &= \frac{1}{2}\partial^\mu\phi_a\partial_\mu\phi_a + \frac{i}{2}\psi^j\tilde{\sigma}^\mu D_\mu\psi_j - \frac{1}{4}g_{AB}^{-2}F^A_{\mu\nu}F^{B\mu\nu} \\ &\quad - \frac{1}{2}y^{ajk}\phi_a(\psi_j\varepsilon\psi_k) - \frac{1}{24}\lambda_{abcd}\phi_a\phi_b\phi_c\phi_d \\ &\quad - \frac{1}{2}\mathrm{m}^{jk}(\psi_j\varepsilon\psi_k) - \frac{1}{2}m^2_{ab}\phi_a\phi_b - \frac{1}{6}h_{abc}\phi_a\phi_b\phi_c \\ &\quad + \mathcal{L}_{\text{gauge-fix}} + \mathcal{L}_{\text{ghost}}, \end{aligned} \tag{A1}$$

featuring real scalar field components ϕ^a, vectors of fermionic Weyl components as well as their conjugates $\psi_i = (\psi^i)^*$ whose spinor indices are contracted by the two-dimensional Levi-Civita ε, as well as gauge fields with the field strength tensors $F^A_{\mu\nu}$ and covariant derivative D_μ. Note the latter do not couple to scalars in accord with our model. Moreover, only the gauge coupling square g^2_{AB}, Yukawa interaction y_{aij}, and scalar quartic coupling λ_{abcd} are relevant, while we will neglect fermionic m^{ij} and scalar masses m^2_{ab} and cubic terms h_{abc}. In the same manner, details of the gauge fixing and Fadeev-Popov ghosts do not play a role. We will make fermionic indices implicit wherever appropriate. Moreover, t^A_{ij} is introduced as the fermionic generator and $(C_2^G)^{AB}$ as the Casimir invariant of the gauge interaction. Moreover, the fermion Casimir and Dynkin index are given by

$$(C_2^F)_{ij} = g^2_{AB}(t^A t^B)_{ij}, \qquad (S_2^F)^{AB} = \mathrm{tr}(t^A t^B). \tag{A2}$$

The quartic β function is composed of external leg and vertex corrections

$$\beta^{abcd}_{\lambda,3\ell} = \gamma^{e(a}_{\phi,3\ell}\lambda^{bcd)e} + \beta^{(abcd)}_{\phi^4,3\ell}. \tag{A3}$$

The gaugeless part of both quantities are given in [53]. In this limit, the leg corrections coincide with the scalar anomalous dimension. For gauge dependent terms, the bases agree only structurally. The reason is that each coefficient may also contain vertex corrections that can be brought to the shape of leg corrections using gauge transformations of tensor structures. For instance, this cancels all gauge dependence of the anomalous dimensions. The gauge interaction terms missing in [53] are of order $\propto y^4g^2$ and $\propto y^2g^4$ and read

$$\begin{aligned}\gamma^{ab}_{\phi,3\ell} &= \gamma^{ab}_{\phi,3\ell}|_{g^2=0} + G_1\mathrm{tr}(y^aC_2^Fy^cy^by^c + y^bC_2^Fy^cy^ay^c) + G_2\mathrm{tr}(y^ay^cC_2^Fy^cy^b) + G_3\mathrm{tr}(y^ay^by^cy^cC_2^F + y^by^ay^cy^cC_2^F) \\ &\quad + G_4\mathrm{tr}(y^aC_2^Fy^by^cy^c) + G_5\mathrm{tr}(y^at^Ay^by^ct^By^c)g^2_{AB} + G_6\mathrm{tr}(y^aC_2^Fy^bC_2^F) + G_7\mathrm{tr}(y^aC_2^FC_2^Fy^b) \\ &\quad + G_8\mathrm{tr}(y^ay^bt^At^B)(g^2S_2^Fg^2)_{AB} + G_9\mathrm{tr}(y^ay^bt^At^B)(g^2C_2^Gg^2)_{AB}. \end{aligned} \tag{A4}$$

Here $G_{1..9}$ are *a priori* unknown coefficients that can be fixed by an actual loop computation. Note that this parametrization assumes $\gamma_{\phi,3\ell}$ to be symmetric, as there is no explicitly broken flavor symmetry in our model.

As for the vertex corrections, we again refer to [53] for the gaugeless tensor structures, and provide the missing ones:

$$\begin{aligned}\beta^{abcd}_{\phi^4,3\ell} &= \beta^{abcd}_{\phi^4,3\ell}|_{g^2=0} + Q_1\lambda^{abef}\lambda^{cdeg}\mathrm{tr}(y^f y^g C_2^F) + Q_2\lambda^{abef}\mathrm{tr}(y^c y^e y^f y^d C_2^F) + Q_3\lambda^{abef}\mathrm{tr}(y^c y^e t^A y^d y^f t^B)g^2_{AB}\\
&+ Q_4\lambda^{abef}\mathrm{tr}(y^c y^e t^A y^f y^d t^B)g^2_{AB} + Q_5\lambda^{abef}\mathrm{tr}(y^c t^A y^e y^f t^B y^d)g^2_{AB} + Q_6\lambda^{abef}\mathrm{tr}(y^c y^e C_2^F y^f y^d)g^2_{AB}\\
&+ Q_7\lambda^{abef}\mathrm{tr}(y^c y^e C_2^F y^d y^f)g^2_{AB} + Q_8\lambda^{abef}\mathrm{tr}(y^c y^e y^f C_2^F y^d)g^2_{AB} + Q_9\mathrm{tr}(y^a y^b y^c y^d C_2^F C_2^F) + Q_{10}\mathrm{tr}(y^a y^b y^c C_2^F y^d C_2^F)\\
&+ Q_{11}\mathrm{tr}(y^a y^b C_2^F y^c y^d C_2^F) + Q_{12}\mathrm{tr}(y^a y^b t^A y^c C_2^F y^d t^B)g^2_{AB} + Q_{13}\mathrm{tr}(y^a t^A C_2^F y^b y^c t^B y^d)g^2_{AB}\\
&+ Q_{14}\mathrm{tr}(y^a t^A y^c t^C y^b t^B y^d)g^2_{AB}g^2_{CD} + Q_{15}\mathrm{tr}(y^a t^A t^C y^b t^B y^c t^D y^d)g^2_{AB}g^2_{CD} + Q_{16}\mathrm{tr}(y^a y^b t^A t^C y^c y^d t^B t^D)g^2_{AB}g^2_{CD}\\
&+ Q_{17}\mathrm{tr}(y^a y^b t^A t^C)\mathrm{tr}(y^c y^d t^B t^D)g^2_{AB}g^2_{CD} + Q_{18}\mathrm{tr}(y^a t^A y^b t^C)\mathrm{tr}(y^c t^B y^d t^D)g^2_{AB}g^2_{CD} + Q_{19}\mathrm{tr}(y^a t^A y^b t^C)\mathrm{tr}(y^c y^d t^B t^D)g^2_{AB}g^2_{CD}\\
&+ Q_{20}\mathrm{tr}(y^a y^b t^A y^c y^d t^B)(g^2 S_2^F g^2)_{AB} + Q_{21}\mathrm{tr}(y^a y^b t^A y^c y^d t^B)(g^2 C_2^G g^2)_{AB} + Q_{22}\mathrm{tr}(y^a y^b y^c t^A y^d t^B)(g^2 S_2^F g^2)_{AB}\\
&+ Q_{23}\mathrm{tr}(y^a y^b y^c t^A y^d t^B)(g^2 C_2^G g^2)_{AB} + Q_{24}\mathrm{tr}(y^a y^b y^c y^d t^A t^B)(g^2 S_2^F g^2)_{AB} + Q_{25}\mathrm{tr}(y^a y^b y^c y^d t^A t^B)(g^2 C_2^G g^2)_{AB}\\
&+ Q_{26}\mathrm{tr}(y^a t^A y^b y^e y^c t^B y^d y^e)g^2_{AB} + Q_{27}\mathrm{tr}(y^a y^b C_2^F y^c y^e y^d y^e) + Q_{28}\mathrm{tr}(y^a y^b y^e t^A y^c y^e y^d t^B)g^2_{AB}\\
&+ Q_{29}\mathrm{tr}(y^a y^b t^A y^e y^c t^B y^d y^e)g^2_{AB} + Q_{30}\mathrm{tr}(y^a y^b y^e y^e y^c y^d C_2^F) + Q_{31}\mathrm{tr}(y^a y^b y^c y^e y^e y^d C_2^F)\\
&+ Q_{32}\mathrm{tr}(y^a t^A y^e y^b t^B y^c y^d y^e)g^2_{AB} + Q_{33}\mathrm{tr}(y^a y^b y^c y^e y^d y^e C_2^F) + Q_{34}\mathrm{tr}(y^a y^b y^e y^c y^d y^e C_2^F) + Q_{35}\mathrm{tr}(y^a y^b y^e y^c C_2^F y^d y^e)\\
&+ Q_{36}\mathrm{tr}(y^a y^b t^A y^c y^e y^e y^d t^B)g^2_{AB} + Q_{37}\mathrm{tr}(y^a t^A y^e y^b y^c t^B y^e y^d)g^2_{AB} + Q_{38}\mathrm{tr}(y^a t^A y^b y^c y^e t^B y^e y^d)g^2_{AB}\\
&+ Q_{39}\mathrm{tr}(y^a t^A y^e y^e y^b y^c t^B y^d)g^2_{AB} + Q_{40}\mathrm{tr}(y^a y^b y^c y^e C_2^F y^d y^e) + Q_{41}\mathrm{tr}(y^a y^b y^c t^A y^d y^e t^B y^e)g^2_{AB}\\
&+ Q_{42}\mathrm{tr}(y^a y^b y^c y^d C_2^F y^e y^e) + Q_{43}\mathrm{tr}(y^a y^b y^c y^d y^e C_2^F y^e),\end{aligned} \tag{A5}$$

where $Q_{1\cdots43}$ are again open coefficients. Note that we do not need to account for any non-naïve influence of γ_5 at this loop order as discussed in Sec. III.

APPENDIX B: FINITE-N BETA FUNCTIONS

Here we present the finite-N corrections to the β functions (14)–(17). Apart from the Veneziano parameter ϵ, these also retain an explicit dependence on inverse powers of the parameter N_c. An extensive analysis of the finite-N conformal window at 2NLO was conducted in [13] (see there for explicit expressions up to 322). In the following, we make use of the abbreviations $r_c \equiv N_c^{-2}$ and $r_f \equiv [(\frac{11}{2}+\epsilon)N_c]^{-2}$ and provide the four-loop gauge beta function

$$\begin{aligned}\alpha_g^{-2}\beta_g^{(4)} &= \left\{\left[-\frac{260}{243}\epsilon^3 + \left(-\frac{56\zeta_3}{3} - \frac{21598}{243}\right)\epsilon^2 + \left(-\frac{1808\zeta_3}{9} - \frac{123473}{324}\right)\epsilon - 550\zeta_3 - \frac{14731}{72}\right] + r_c\left[\left(\frac{128\zeta_3}{9} + \frac{7495}{243}\right)\epsilon^2\right.\right.\\
&\left. + \left(\frac{2504\zeta_3}{9} + \frac{71765}{324}\right)\epsilon + 396\zeta_3 + \frac{154\epsilon^3}{243} + \frac{30047}{72}\right] + r_c^2\left[\left(\frac{623}{27} - \frac{488\zeta_3}{9}\right)\epsilon^2 + \left(\frac{29753}{108} - \frac{5456\zeta_3}{9}\right)\epsilon\right.\\
&\left.\left. - 1694\zeta_3 + \frac{19613}{24}\right] + r_c^3\left[\frac{23\epsilon}{4} + \frac{253}{8}\right]\right\}\alpha_g^3 + \left\{\left[\left(36\zeta_3 + \frac{8017}{36}\right)\epsilon^2 + \left(396\zeta_3 + \frac{38797}{72}\right)\epsilon + 1089\zeta_3\right.\right.\\
&\left. + \frac{379\epsilon^3}{18} - \frac{12947}{48}\right] + r_c\left[\left(-54\zeta_3 - \frac{1184}{9}\right)\epsilon^2 + \left(-594\zeta_3 - \frac{45749}{72}\right)\epsilon - \frac{3267\zeta_3}{2} - \frac{161\epsilon^3}{18} - \frac{24079}{24}\right]\\
&+ r_c^2\left[\left(18\zeta_3 - \frac{3}{4}\right)\epsilon^2 + \left(198\zeta_3 - \frac{33}{4}\right)\epsilon + \frac{1089\zeta_3}{2} - \frac{363}{16}\right]\Big\}\alpha_g^2\alpha_y + \left\{\left[\left(\frac{1659}{4} - 12\zeta_3\right)\epsilon^2 + (2475 - 132\zeta_3)\epsilon\right.\right.\\
&\left. - 363\zeta_3 + 23\epsilon^3 + \frac{78287}{16}\right] + r_c\left[\left(12\zeta_3 + \frac{89}{4}\right)\epsilon^2 + (132\zeta_3 + 154)\epsilon + 363\zeta_3 + \epsilon^3 + \frac{5445}{16}\right]\Big\}\alpha_g\alpha_y^2\\
&+ \left\{\left[-\frac{11\epsilon^4}{3} - 100\epsilon^3 - 986\epsilon^2 - \frac{25267\epsilon}{6} - \frac{105875}{16}\right] + r_c\left[\left(\frac{7}{3} - 6\zeta_3\right)\epsilon^2 + \left(\frac{77}{3} - 66\zeta_3\right)\epsilon - \frac{363\zeta_3}{2} + \frac{847}{12}\right]\right\}\alpha_y^3\\
&+ \left\{\left[-10\epsilon^3 - 165\epsilon^2 - \frac{1815\epsilon}{2} - \frac{6655}{4}\right] - r_c[55 + 10\epsilon]\right\}\alpha_y^2\alpha_u - r_c[20\epsilon + 110]\alpha_y^2\alpha_v\\
&+ \{[12\epsilon^2 + 132\epsilon + 363] + 12r_c\}\alpha_y\alpha_u^2 + 48r_c\alpha_y\alpha_u\alpha_v + 12r_c[1 + r_f]\alpha_y\alpha_v^2.\end{aligned} \tag{B1}$$

Because of subleading corrections absent in the large-N limit, the double-trace quartic α_v makes a direct appearance in the gauge four-loop β function. The same happens for the three-loop expressions of the Yukawa

$$\begin{aligned}\alpha_y^{-1}\beta_y^{(3)} = &\left\{\left[-\frac{3\epsilon^3}{8}+\frac{59\epsilon^2}{16}+\frac{2595\epsilon}{32}+\frac{17413}{64}\right]+r_c[(6\zeta_3-28)\epsilon+39\zeta_3-162]\right\}\alpha_y^3+\left\{\left[-19\epsilon^2-\frac{445\epsilon}{2}-649\right]\right.\\&\left.+r_c\left[19\epsilon^2+\frac{445\epsilon}{2}+633\right]+16r_c^2\right\}\alpha_g\alpha_y^2+\left\{\left[\left(-36\zeta_3-\frac{893}{8}\right)\epsilon-198\zeta_3-17\epsilon^2-\frac{1217}{16}\right]+r_c[(54\zeta_3+92)\epsilon\right.\\&\left.+279\zeta_3+17\epsilon^2+31]+r_c^2\left[\left(\frac{157}{8}-18\zeta_3\right)\epsilon-81\zeta_3+\frac{721}{16}\right]\right\}\alpha_g^2\alpha_y+\left\{\left[\left(24\zeta_3+\frac{649}{9}\right)\epsilon+132\zeta_3+\frac{70\epsilon^2}{27}\right.\right.\\&\left.\left.+\frac{641}{6}\right]+r_c\left[-\frac{70\epsilon^2}{27}-\frac{856\epsilon}{9}-\frac{2413}{12}\right]+r_c^2[(23-24\zeta_3)\epsilon-132\zeta_3+62]+\frac{129}{4}r_c^3\right\}\alpha_g^3+\left\{[12\epsilon^2+162\epsilon+528]\right.\\&\left.+60r_c+30\left(\frac{11}{2}+\epsilon\right)r_f\right\}\alpha_y^2\alpha_u+\left\{48r_c+60\left(\frac{11}{2}+\epsilon\right)r_f+24r_cr_f\right\}\alpha_y^2\alpha_v+\left\{\left[5\epsilon+\frac{25}{2}\right]\right.\\&\left.+r_f\left[85\epsilon+\frac{905}{2}\right]\right\}\alpha_y\alpha_u^2+\{r_f[100\epsilon+490]+r_f^2[80\epsilon+440]\}\alpha_y\alpha_u\alpha_v+\left\{r_f\left[5\epsilon+\frac{25}{2}\right]+r_f^2\left[85\epsilon+\frac{905}{2}\right]\right\}\alpha_y\alpha_v^2\\&-\{8+32r_f\}\alpha_u^3-\{84r_f+36r_f^2\}\alpha_u^2\alpha_v-\{24r_f+96r_f^2\}\alpha_u\alpha_v^2-\{4r_f+20r_f^2+16r_f^3\}\alpha_v^3\\&+\left\{4\left[\frac{11}{2}+\epsilon\right][1-r_c][1+r_f]\right\}\alpha_g\alpha_y\alpha_u+\left\{8\left[\frac{11}{2}+\epsilon\right][r_f-r_cr_f]\right\}\alpha_g\alpha_y\alpha_v,\end{aligned}\tag{B2}$$

as well as the single-trace coupling

$$\begin{aligned}\beta_u^{(3)} = &\{104+r_f[1152\zeta_3+2360]\}\alpha_u^4+\{r_f[1536\zeta_3+2912]+r_f^2[6144\zeta_3+6752]\}\alpha_u^3\alpha_v-\{280r_f-r_f^2[9216\zeta_3\\&+12728]\}\alpha_u^2\alpha_v^2-\{104r_f-r_f^2[768\zeta_3+1472]-r_f^3[5376\zeta_3+6568]\}\alpha_u\alpha_v^3+\{34+226r_f\}\alpha_y\alpha_u^3+648r_f\alpha_y\alpha_u^2\alpha_v\\&+\{66r_f+642r_f^2\}\alpha_y\alpha_u\alpha_v^2+\{[166\epsilon+889]+r_f[(216\zeta_3+156)\epsilon+1188\zeta_3+858]\}\alpha_y^2\alpha_u^2+\{r_f[(192\zeta_3+734)\epsilon\\&+1056\zeta_3+3965]\}\alpha_y^2\alpha_u\alpha_v+\{r_f[64\epsilon+352]+r_f^2[(216\zeta_3+136)\epsilon+1188\zeta_3+748]\}\alpha_y^2\alpha_v^2+\left\{\left[-\frac{315\epsilon^2}{4}-\frac{3209\epsilon}{4}\right.\right.\\&\left.\left.-\frac{32483}{16}\right]+r_c[12\zeta_3-168]\right\}\alpha_y^3\alpha_u-\left\{r_c[152+96\zeta_3]-64\left[\frac{11}{2}+\epsilon\right]r_f\right\}\alpha_y^3\alpha_v+\left\{\left[\frac{13\epsilon^3}{4}+\frac{265\epsilon^2}{8}+\frac{1111\epsilon}{16}-\frac{2541}{32}\right]\right.\\&\left.+r_c[(20-24\zeta_3)\epsilon-132\zeta_3+110]\right\}\alpha_y^4+\left\{\left[(24\zeta_3-5)\epsilon^2+(264\zeta_3-55)\epsilon+726\zeta_3-\frac{605}{4}\right]+r_c\left[(5-24\zeta_3)\epsilon^2\right.\right.\\&\left.\left.+(55-264\zeta_3)\epsilon-726\zeta_3+\frac{605}{4}\right]\right\}\alpha_g\alpha_y^3+\left\{\left[\left(\frac{149}{2}-120\zeta_3\right)\epsilon-660\zeta_3+\frac{1639}{4}\right]+r_c\left[\left(120\zeta_3-\frac{149}{2}\right)\epsilon+660\zeta_3\right.\right.\\&\left.\left.-\frac{1639}{4}\right]\right\}\alpha_g\alpha_y^2\alpha_u+\{r_f[(112-144\zeta_3)\epsilon-792\zeta_3+616]+r_cr_f[(144\zeta_3-112)\epsilon+792\zeta_3-616]\}\alpha_g\alpha_y^2\alpha_v\\&+\{[96\zeta_3-102][1-r_c]\}\alpha_g\alpha_y\alpha_u^2+\left\{r_f[288\zeta_3-306]+r_f^2\left[(306-288\zeta_3)\epsilon^2+(3366-3168\zeta_3)\epsilon-8712\zeta_3\right.\right.\\&\left.\left.+\frac{18513}{2}\right]\right\}\alpha_g\alpha_y\alpha_u\alpha_v+\left\{\left[5\epsilon^2+\frac{133\epsilon}{4}+\frac{253}{8}\right]+r_c\left[(24\zeta_3-66)\epsilon+132\zeta_3-5\epsilon^2-\frac{847}{4}\right]+r_c^2\left[\left(\frac{131}{4}-24\zeta_3\right)\epsilon\right.\right.\\&\left.\left.-132\zeta_3+\frac{1441}{8}\right]\right\}\alpha_g^2\alpha_y^2+\left\{\left[\frac{13}{4}-8\epsilon\right]+r_c\left[-36\zeta_3+8\epsilon+\frac{53}{2}\right]+r_c^2\left[36\zeta_3-\frac{119}{4}\right]\right\}\alpha_g^2\alpha_y\alpha_u.\end{aligned}\tag{B3}$$

Moreover, the three-loop β function

$$\begin{aligned}\beta_v^{(3)} &= \{[384\zeta_3+772]+r_f[1536\zeta_3+1700]\}\alpha_u^4+\{480+r_f[4608\zeta_3+9600]\}\alpha_u^3\alpha_v\\
&+\{12+r_f[1152\zeta_3+6680]+r_f^2[8064\zeta_3+10476]\}\alpha_u^2\alpha_v^2+\{1264r_f+r_f^2[6144\zeta_3+10544]\}\alpha_u\alpha_v^3\\
&+\{132r_f+r_f^2[960\zeta_3+1844]+r_f^3[2112\zeta_3+2960]\}\alpha_v^4+192\alpha_y\alpha_u^3+\{66+642r_f\}\alpha_y\alpha_u^2\alpha_v\\
&+648r_f\alpha_y\alpha_u\alpha_v^2+\{130r_f+322r_f^2\}\alpha_y\alpha_v^3+\left[(192\zeta_3+187)\epsilon+1056\zeta_3+\frac{1985}{2}\right]\alpha_y^2\alpha_u^2\\
&+\{[(96\zeta_3+152)\epsilon+528\zeta_3+788]+r_f[(528\zeta_3+132)\epsilon+2904\zeta_3+726]\}\alpha_y^2\alpha_u\alpha_v\\
&+\left\{\left[41\epsilon+\frac{427}{2}\right]+r_f[(192\zeta_3+268)\epsilon+1056\zeta_3+1426]\right\}\alpha_y^2\alpha_v^2+[(-96\zeta_3-88)\epsilon^2\\
&+(-1056\zeta_3-904)\epsilon-2904\zeta_3-2310]\alpha_y^3\alpha_u+\left\{\left[-\frac{187\epsilon^2}{4}-\frac{1801\epsilon}{4}-\frac{16995}{16}\right]+r_c[12\zeta_3-136]\right\}\alpha_y^3\alpha_v\\
&+\left[-10\epsilon^3-183\epsilon^2-\frac{2211\epsilon}{2}-\frac{8833}{4}\right]\alpha_y^4+\left\{\left[(24\zeta_3-2)\epsilon^2+(264\zeta_3-22)\epsilon+726\zeta_3-\frac{121}{2}\right]\right.\\
&\left.+r_c\left[(2-24\zeta_3)\epsilon^2+(22-264\zeta_3)\epsilon-726\zeta_3+\frac{121}{2}\right]\right\}\alpha_g\alpha_y^3+\{[(112-144\zeta_3)\epsilon\\
&-792\zeta_3+616][1-r_c]\}\alpha_g\alpha_y^2\alpha_u+\left\{\left[\left(\frac{149}{2}-120\zeta_3\right)\epsilon-660\zeta_3+\frac{1639}{4}\right][1-r_c]\right\}\alpha_g\alpha_y^2\alpha_v\\
&+\{[144\zeta_3-153][1-r_c]\}\alpha_g\alpha_y\alpha_u^2+\left\{[48\zeta_3-51]+r_f\left[(51-48\zeta_3)\epsilon^2+(561-528\zeta_3)\epsilon\right.\right.\\
&\left.\left.-1260\zeta_3+\frac{5355}{4}\right]+r_f^2[(204-192\zeta_3)\epsilon^2+(2244-2112\zeta_3)\epsilon-5808\zeta_3+6171]\right\}\alpha_g\alpha_y\alpha_v^2\\
&+\{[192\zeta_3-204][1-r_c]\}\alpha_g\alpha_y\alpha_u\alpha_v+\{[24\epsilon^2+264\epsilon+726][1-r_c]\}\alpha_g^2\alpha_y^2\\
&+\left\{\left[\frac{13}{4}-8\epsilon\right]+r_c\left[-36\zeta_3+8\epsilon+\frac{53}{2}\right]+r_c^2\left[36\zeta_3-\frac{119}{4}\right]\right\}\alpha_g^2\alpha_y\alpha_v \qquad \text{(B4)}\end{aligned}$$

ceases to be just quadratic in α_v due to a subleading correction in N.

APPENDIX C: GAUGE-DEPENDENT ANOMALOUS DIMENSIONS

In this appendix, we provide results for the gauge-dependent field strength anomalous dimensions of fermions ψ, gauge fields A_μ, as well as their ghosts c, using the definition (23). We have computed these explicitly with R_ξ gauge fixing, such that $\xi=1$ corresponds to the 't Hooft–Feynman gauge. The scalar field anomalous dimension is gauge independent and provided in (24). The fermionic field anomalous dimension reads

$$\begin{aligned}\gamma_\psi^{(1)} &= \frac{1}{2}\xi\alpha_g+\frac{1}{4}(11+2\epsilon)\alpha_y,\\
\gamma_\psi^{(2)} &= \frac{1}{8}(\xi^2+8\xi-4\epsilon)\alpha_g^2-\frac{1}{2}(11+2\epsilon)\alpha_y\alpha_g-\frac{1}{32}(23+2\epsilon)(11+2\epsilon)\alpha_y^2,\\
\gamma_\psi^{(3)} &= -\frac{11}{8}(11+2\epsilon)\alpha_u^2\alpha_y+\frac{1}{2}(11+2\epsilon)^2\alpha_u\alpha_y^2+\left(\frac{13387}{256}+\frac{2119}{128}\epsilon+\frac{49}{64}\epsilon^2-\frac{3}{32}\epsilon^3\right)\alpha_y^3\\
&+\frac{1}{32}(11+2\epsilon)(137+48\zeta_3+24\epsilon)\alpha_y^2\alpha_g+\frac{1}{64}(11+2\epsilon)(77-192\zeta_3+12\epsilon)\alpha_y\alpha_g^2\\
&+\left[-\frac{331}{32}-\frac{21}{16}\zeta_3-\left(\frac{111}{64}-\frac{3}{8}\zeta_3\right)\xi+\left(\frac{39}{64}+\frac{3}{16}\zeta_3\right)\xi^2+\frac{5}{32}\xi^3-\left(\frac{109}{24}+\frac{17}{16}\xi\right)\epsilon+\frac{5}{18}\epsilon^2\right]\alpha_g^3. \qquad \text{(C1)}\end{aligned}$$

The gauge field anomalous dimension is

$$\gamma_A^{(1)} = \frac{1}{6}(9+3\xi+4\epsilon)\alpha_g,$$
$$\gamma_A^{(2)} = \frac{1}{8}(95+11\xi+2\xi^2+28\epsilon)\alpha_g^2 - \frac{1}{4}(11+2\epsilon)^2\alpha_y\alpha_g,$$
$$\gamma_A^{(3)} = \frac{1}{8}(11+2\epsilon)^2(20+3\epsilon)\alpha_y^2\alpha_g - \frac{31}{32}(11+2\epsilon)^2\alpha_g^2\alpha_y + \left[\frac{2039}{96} - \frac{255}{16}\zeta_3 - \left(\frac{9}{32} - \frac{3}{4}\zeta_3\right)\xi + \left(\frac{33}{32} + \frac{3}{16}\zeta_3\right)\xi^2 + \frac{7}{32}\xi^3 - \left(\frac{347}{72} + 3\zeta_3 + \xi\right)\epsilon - \frac{49}{18}\epsilon^2\right]\alpha_g^3, \quad \text{(C2)}$$

and the corresponding ghost has

$$\gamma_c^{(1)} = -\frac{1}{4}(3-\xi)\alpha_g,$$
$$\gamma_c^{(2)} = \frac{1}{48}(15-3\xi+20\epsilon)\alpha_g^2,$$
$$\gamma_c^{(3)} = -\frac{23}{64}(11+2\epsilon)^2\alpha_g^2\alpha_y + \left[\frac{3569}{192} + \frac{255}{32}\zeta_3 - \frac{1}{8}(15+3\zeta_3)\xi + \frac{3}{32}(1-\zeta_3)\xi^2 + \frac{3}{64}\xi^3 + \left(\frac{983}{144} + \frac{3}{2}\zeta_3 - \frac{7}{16}\xi\right)\epsilon + \frac{35}{108}\epsilon^2\right]\alpha_g^3. \quad \text{(C3)}$$

As the overall renormalization of the gauge-fixing term cancels, the β function of the gauge parameter reads

$$\beta_\xi = -2\xi\gamma_A. \quad \text{(C4)}$$

We observe that (C4) has two types of fixed points due to either the Landau gauge ($\xi^* = 0$) or the vanishing of the gauge field anomalous dimension ($\gamma_A = 0$). The latter happens at

$$\xi^* = -3 + 2.28\epsilon + 10.19\epsilon^2 + 21.92\epsilon^3 + \mathcal{O}(\epsilon^4). \quad \text{(C5)}$$

Moreover, we note that the critical exponent of the flow (C4) at the fixed point (C5)

$$\left.\frac{\partial\beta_\xi}{\partial\xi}\right|_{\xi=\xi^*} = 1.368\epsilon + 1.146\epsilon^2 + 13.83\epsilon^3 + \mathcal{O}(\epsilon^4) \quad \text{(C6)}$$

is manifestly positive. Hence, we conclude that the Landau gauge corresponds to an UV fixed point of the flow (C4), whereas a vanishing gauge field anomalous dimension corresponds to an IR attractive fixed point.

[1] D. J. Gross and F. Wilczek, Ultraviolet Behavior of Non-Abelian Gauge Theories, Phys. Rev. Lett. **30**, 1343 (1973).
[2] H. D. Politzer, Reliable Perturbative Results for Strong Interactions?, Phys. Rev. Lett. **30**, 1346 (1973).
[3] D. F. Litim and F. Sannino, Asymptotic safety guaranteed, J. High Energy Phys. 12 (2014) 178.
[4] A. D. Bond and D. F. Litim, Theorems for asymptotic safety of gauge theories, Eur. Phys. J. C **77**, 429 (2017).
[5] A. D. Bond and D. F. Litim, Price of Asymptotic Safety, Phys. Rev. Lett. **122**, 211601 (2019).
[6] A. D. Bond and D. F. Litim, More asymptotic safety guaranteed, Phys. Rev. D **97**, 085008 (2018).
[7] A. D. Bond and D. F. Litim, Asymptotic Safety Guaranteed in Supersymmetry, Phys. Rev. Lett. **119**, 211601 (2017).
[8] A. D. Bond, D. F. Litim, G. Medina Vazquez, and T. Steudtner, UV conformal window for asymptotic safety, Phys. Rev. D **97**, 036019 (2018).
[9] A. Bond and D. F. Litim, Interacting ultraviolet completions of four-dimensional gauge theories, Proc. Sci. LATTICE2016 (**2017**) 208.
[10] T. Buyukbese and D. F. Litim, Asymptotic safety of gauge theories beyond marginal interactions, Proc. Sci. LATTICE2016 (**2017**) 233.
[11] A. D. Bond, D. F. Litim, and T. Steudtner, Asymptotic safety with Majorana fermions and new large N equivalences, Phys. Rev. D **101**, 045006 (2020).
[12] D. F. Litim and T. Steudtner, ARGES—advanced renormalisation group equation simplifier, Comput. Phys. Commun. **265**, 108021 (2021).
[13] A. D. Bond, D. F. Litim, and G. M. Vazquez, Conformal windows beyond asymptotic freedom, Phys. Rev. D **104**, 105002 (2021).
[14] A. D. Bond and D. F. Litim, Asymptotic safety guaranteed for strongly coupled gauge theories, Phys. Rev. D **105**, 105005 (2022).
[15] D. Bailin and A. Love, Asymptotic near freedom, Nucl. Phys. **B75**, 159 (1974).
[16] S. Weinberg, Ultraviolet divergences in quantum theories of gravitation, in *General Relativity: An Einstein Centenary Survey* (Cambridge University Press, Cambridge, UK, 1980), pp. 790–831.
[17] D. F. Litim, M. Mojaza, and F. Sannino, Vacuum stability of asymptotically safe gauge-Yukawa theories, J. High Energy Phys. 01 (2016) 081.
[18] F. Sannino and I. M. Shoemaker, Asymptotically safe dark matter, Phys. Rev. D **92**, 043518 (2015).

[19] N. G. Nielsen, F. Sannino, and O. Svendsen, Inflation from asymptotically safe theories, Phys. Rev. D **91**, 103521 (2015).

[20] D. H. Rischke and F. Sannino, Thermodynamics of asymptotically safe theories, Phys. Rev. D **92**, 065014 (2015).

[21] A. Codello, K. Langæble, D. F. Litim, and F. Sannino, Conformal Gauge-Yukawa theories away from four dimensions, J. High Energy Phys. 07 (2016) 118.

[22] A. D. Bond, G. Hiller, K. Kowalska, and D. F. Litim, Directions for model building from asymptotic safety, J. High Energy Phys. 08 (2017) 004.

[23] N. A. Dondi, V. Prochazka, and F. Sannino, Conformal data of fundamental gauge-Yukawa theories, Phys. Rev. D **98**, 045002 (2018).

[24] K. Kowalska, A. Bond, G. Hiller, and D. Litim, Towards an asymptotically safe completion of the standard model, Proc. Sci. EPS-HEP2017 (**2017**) 542.

[25] S. Abel and F. Sannino, Radiative symmetry breaking from interacting UV fixed points, Phys. Rev. D **96**, 056028 (2017).

[26] N. Christiansen, A. Eichhorn, and A. Held, Is scale-invariance in gauge-Yukawa systems compatible with the graviton?, Phys. Rev. D **96**, 084021 (2017).

[27] F. Sannino and V. Skrinjar, Instantons in asymptotically safe and free quantum field theories, Phys. Rev. D **99**, 085010 (2019).

[28] D. Barducci, M. Fabbrichesi, C. M. Nieto, R. Percacci, and V. Skrinjar, In search of a UV completion of the standard model—378,000 models that don't work, J. High Energy Phys. 11 (2018) 057.

[29] G. Hiller, C. Hormigos-Feliu, D. F. Litim, and T. Steudtner, Anomalous magnetic moments from asymptotic safety, Phys. Rev. D **102**, 071901 (2020).

[30] G. Hiller, C. Hormigos-Feliu, D. F. Litim, and T. Steudtner, Asymptotically safe extensions of the standard model with flavour phenomenology, in *54th Rencontres de Moriond on Electroweak Interactions and Unified Theories* (ARISF, 2019), pp. 415–418, arXiv:1905.11020.

[31] G. Hiller, C. Hormigos-Feliu, D. F. Litim, and T. Steudtner, Model building from asymptotic safety with Higgs and flavor portals, Phys. Rev. D **102**, 095023 (2020).

[32] S. Bißmann, G. Hiller, C. Hormigos-Feliu, and D. F. Litim, Multi-lepton signatures of vector-like leptons with flavor, Eur. Phys. J. C **81**, 101 (2021).

[33] R. Bause, G. Hiller, T. Höhne, D. F. Litim, and T. Steudtner, B-anomalies from flavorful U(1)′ extensions, safely, Eur. Phys. J. C **82**, 42 (2022).

[34] G. Hiller, D. F. Litim, and K. Moch, Fixed points in supersymmetric extensions of the standard model, Eur. Phys. J. C **82**, 952 (2022).

[35] G. Hiller, T. Höhne, D. F. Litim, and T. Steudtner, Portals into Higgs vacuum stability, Phys. Rev. D **106**, 115004 (2022).

[36] G. Hiller, T. Höhne, D. F. Litim, and T. Steudtner, Vacuum stability as a guide for model buisldling, in *57th Rencontres de Moriond on Electroweak Interactions and Unified Theories* (2023), 5, arXiv:2305.18520.

[37] L. Del Debbio, The conformal window on the lattice, Proc. Sci. Lattice2010 (**2014**) 004.

[38] L. Di Pietro and M. Serone, Looking through the QCD conformal window with perturbation theory, J. High Energy Phys. 07 (2020) 049.

[39] Y. Kluth, D. F. Litim, and M. Reichert, Spectral functions of gauge theories with Banks-Zaks fixed points, Phys. Rev. D **107**, 025011 (2023).

[40] A. Bednyakov and A. Pikelner, Four-Loop Gauge and Three-Loop Yukawa Beta Functions in a General Renormalizable Theory, Phys. Rev. Lett. **127**, 041801 (2021).

[41] J. Davies, F. Herren, and A. E. Thomsen, General gauge-Yukawa-quartic β-functions at 4-3-2-loop order, J. High Energy Phys. 01 (2022) 051.

[42] G. Veneziano, Some aspects of a unified approach to gauge, dual and Gribov theories, Nucl. Phys. **B117**, 519 (1976).

[43] G. 't Hooft, A planar diagram theory for strong interactions, Nucl. Phys. **B72**, 461 (1974).

[44] W. E. Caswell, Asymptotic Behavior of Non-Abelian Gauge Theories to Two Loop Order, Phys. Rev. Lett. **33**, 244 (1974).

[45] T. Banks and A. Zaks, On the phase structure of vector-like gauge theories with massless fermions, Nucl. Phys. **B196**, 189 (1982).

[46] C. Poole and A. E. Thomsen, Constraints on 3- and 4-loop β-functions in a general four-dimensional quantum field theory, J. High Energy Phys. 09 (2019) 055.

[47] A. Valenti and L. Vecchi, Perturbative running of the topological angles, J. High Energy Phys. 01 (2023) 131.

[48] M. E. Machacek and M. T. Vaughn, Two-loop renormalization group equations in a general quantum field theory: (III). Scalar quartic couplings, Nucl. Phys. **B249**, 70 (1985).

[49] M. Luo, H. Wang, and Y. Xiao, Two-loop renormalization group equations in general gauge field theories, Phys. Rev. D **67**, 065019 (2003).

[50] A. E. Thomsen, Introducing RGBeta: A Mathematica package for the evaluation of renormalization group β-functions, Eur. Phys. J. C **81**, 408 (2021).

[51] T. Steudtner, FoRGEr (unpublished).

[52] T. Steudtner, General scalar renormalisation group equations at three-loop order, J. High Energy Phys. 12 (2020) 012.

[53] T. Steudtner, Towards general scalar-Yukawa renormalisation group equations at three-loop order, J. High Energy Phys. 05 (2021) 060.

[54] J. Brod, E. Stamou, and T. Steudtner, MaRTIn (unpublished).

[55] P. Nogueira, Automatic Feynman graph generation, J. Comput. Phys. **105**, 279 (1993).

[56] J. Kuipers, T. Ueda, J. A. M. Vermaseren, and J. Vollinga, FORM version 4.0, Comput. Phys. Commun. **184**, 1453 (2013).

[57] M. Misiak and M. Munz, Two loop mixing of dimension five flavor changing operators, Phys. Lett. B **344**, 308 (1995).

[58] K. G. Chetyrkin, M. Misiak, and M. Munz, Beta functions and anomalous dimensions up to three loops, Nucl. Phys. **B518**, 473 (1998).

[59] K. Chetyrkin and M. Zoller, Three-loop β-functions for top-Yukawa and the Higgs self-interaction in the standard model, J. High Energy Phys. 06 (2012) 033.

[60] R. N. Lee, Presenting LiteRed: A tool for the Loop InTEgrals REDuction, arXiv:1212.2685.

[61] R. N. Lee, LiteRed 1.4: A powerful tool for reduction of multiloop integrals, J. Phys. Conf. Ser. **523**, 012059 (2014).
[62] C. Bobeth, M. Misiak, and J. Urban, Photonic penguins at two loops and m_t dependence of $BR[B \to X_s l^+ l^-]$, Nucl. Phys. **B574**, 291 (2000).
[63] S. P. Martin and D. G. Robertson, Evaluation of the general 3-loop vacuum Feynman integral, Phys. Rev. D **95**, 016008 (2017).
[64] F. Jegerlehner, Facts of life with γ_5, Eur. Phys. J. C **18**, 673 (2001).
[65] C. Poole and A. Thomsen, Weyl Consistency Conditions and γ_5, Phys. Rev. Lett. **123**, 041602 (2019).
[66] J. Davies, F. Herren, C. Poole, M. Steinhauser, and A. E. Thomsen, Gauge Coupling β Functions to Four-Loop Order in the Standard Model, Phys. Rev. Lett. **124**, 071803 (2020).
[67] A. Bednyakov, A. Pikelner, and V. Velizhanin, Yukawa coupling beta-functions in the standard model at three loops, Phys. Lett. B **722**, 336 (2013).
[68] A. Bednyakov, A. Pikelner, and V. Velizhanin, Three-loop SM beta-functions for matrix Yukawa couplings, Phys. Lett. B **737**, 129 (2014).
[69] F. Herren, L. Mihaila, and M. Steinhauser, Gauge and Yukawa coupling beta functions of two-Higgs-doublet models to three-loop order, Phys. Rev. D **97**, 015016 (2018).
[70] I. Jack and H. Osborn, Scheme dependence and multiple couplings, arXiv:1606.02571.
[71] F. Herren and A. E. Thomsen, On ambiguities and divergences in perturbative renormalization group functions, J. High Energy Phys. 06 (2021) 116.
[72] M. E. Machacek and M. T. Vaughn, Two-loop renormalization group equations in a general quantum field theory: (I). Wave function renormalization, Nucl. Phys. **B222**, 83 (1983).
[73] M. E. Machacek and M. T. Vaughn, Two-loop renormalization group equations in a general quantum field theory (II). Yukawa couplings, Nucl. Phys. **B236**, 221 (1984).
[74] A. Pickering, J. Gracey, and D. Jones, Three loop gauge β-function for the most general single gauge-coupling theory, Phys. Lett. B **510**, 347 (2001).
[75] L. Mihaila, Three-loop gauge beta function in non-simple gauge groups, Proc. Sci. RADCOR2013 (**2013**) 060.
[76] I. Schienbein, F. Staub, T. Steudtner, and K. Svirina, Revisiting RGEs for general gauge theories, Nucl. Phys. **B939**, 1 (2019).
[77] A. Bednyakov, A. Pikelner, and V. Velizhanin, Higgs self-coupling beta-function in the standard model at three loops, Nucl. Phys. **B875**, 552 (2013).
[78] K. Chetyrkin and M. Zoller, β-function for the Higgs self-interaction in the standard model at three-loop level, J. High Energy Phys. 04 (2013) 091.
[79] A. Bednyakov, A. Pikelner, and V. Velizhanin, Three-loop Higgs self-coupling beta-function in the standard model with complex Yukawa matrices, Nucl. Phys. **B879**, 256 (2014).
[80] N. Zerf, P. Marquard, R. Boyack, and J. Maciejko, Critical behavior of the QED_3-Gross-Neveu-Yukawa model at four loops, Phys. Rev. B **98**, 165125 (2018).
[81] J. A. Gracey, The QCD beta function at O(1/N(f)), Phys. Lett. B **373**, 178 (1996).
[82] T. Luthe, A. Maier, P. Marquard, and Y. Schröder, Towards the five-loop Beta function for a general gauge group, J. High Energy Phys. 07 (2016) 127.
[83] P. A. Baikov, K. G. Chetyrkin, and J. H. Kühn, Five-Loop Running of the QCD Coupling Constant, Phys. Rev. Lett. **118**, 082002 (2017).
[84] F. Herzog, B. Ruijl, T. Ueda, J. Vermaseren, and A. Vogt, The five-loop beta function of yang-mills theory with fermions, J. High Energy Phys. 02 (2017) 090.
[85] T. Luthe, A. Maier, P. Marquard, and Y. Schröder, The five-loop beta function for a general gauge group and anomalous dimensions beyond feynman gauge, J. High Energy Phys. 10 (2017) 166.
[86] K. G. Chetyrkin, G. Falcioni, F. Herzog, and J. A. M. Vermaseren, Five-loop renormalisation of QCD in covariant gauges, J. High Energy Phys. 10 (2017) 179.
[87] A. Bednyakov and A. Pikelner, Six-loop beta functions in general scalar theory, J. High Energy Phys. 04 (2021) 233.
[88] T. Steudtner, Asymptotic safety: From perturbatively exact models to particle physics, Ph.D. thesis, Sussex U., 2020.
[89] S. Laporta, High precision epsilon expansions of massive four loop vacuum bubbles, Phys. Lett. B **549**, 115 (2002).
[90] Y. Schroder, Automatic reduction of four loop bubbles, Nucl. Phys. B, Proc. Suppl. **116**, 402 (2003).
[91] M. Czakon, The four-loop QCD *beta*-function and anomalous dimensions, Nucl. Phys. **B710**, 485 (2005).
[92] Y. Schroder and A. Vuorinen, High-precision epsilon expansions of single-mass-scale four-loop vacuum bubbles, J. High Energy Phys. 06 (2005) 051.
[93] T. Luthe, Fully massive vacuum integrals at 5 loops, Ph.D. thesis, Bielefeld U., 2015.
[94] A. Pikelner, FMFT: Fully massive four-loop tadpoles, Comput. Phys. Commun. **224**, 282 (2018).
[95] E. Pomoni and L. Rastelli, Large N field theory and AdS tachyons, J. High Energy Phys. 04 (2009) 020.
[96] S. P. Martin and M. T. Vaughn, Two-loop renormalization group equations for soft supersymmetry-breaking couplings, Phys. Rev. D **50**, 2282 (1994).
[97] A. Paterson, Coleman-Weinberg symmetry breaking in the chiral $SU(N) \times SU(N)$ linear σ model, Nucl. Phys. **B190**, 188 (1981).
[98] F. Benini, C. Iossa, and M. Serone, Conformality Loss, Walking, and 4D Complex Conformal Field Theories at Weak Coupling, Phys. Rev. Lett. **124**, 051602 (2020).
[99] S. Weinberg, Phenomenological Lagrangians, Physica (Amsterdam) **96A**, 327 (1979).
[100] D. F. Litim, N. Riyaz, E. Stamou, and T. Steudtner (to be published).
[101] M. A. Luty, J. Polchinski, and R. Rattazzi, The a-theorem and the asymptotics of 4D quantum field theory, J. High Energy Phys. 01 (2013) 152.
[102] G. Mack, All unitary ray representations of the conformal group SU(2,2) with positive energy, Commun. Math. Phys. **55**, 1 (1977).

[103] G. Aarts *et al.*, Phase transitions in particle physics—results and perspectives from lattice quantum chromo-Dynamics, Prog. Part. Nucl. Phys. **133**, 104070 (2023).

[104] J. L. Cardy, *Scaling and Renormalization in Statistical Physics* (Cambridge University Press, Cambridge, England, 1996).

[105] A. Codello, M. Safari, G. P. Vacca, and O. Zanusso, Functional perturbative RG and CFT data in the ϵ-expansion, Eur. Phys. J. C **78**, 30 (2018).

[106] Z. Li and D. Poland, Searching for gauge theories with the conformal bootstrap, J. High Energy Phys. 03 (2021) 172.